Department of Construction Sciences
Solid Mechanics

ISRN LUTFD2/TFHF-14/5189-SE(1-71)

Parameter study on nonlinear piping systems exposed to time history loading in ANSYS

Master's Dissertation by

Stefan Alkmyr

Supervisors:

M.Sc. Jimmy Carlsson, ÅF-Industry AB

Associate Professor Håkan Hallberg, Div. of Solid Mechanics

Examiner:

Associate Professor Mathias Wallin, Div. of Solid Mechanics

Printed by Media-Tryck AB, Lund, Sweden
For information, address:
Division of Solid Mechanics, Lund University, Box 118, SE-221 00 Lund, Sweden
Webpage: www.solid.lth.se

Acknowledgement

This Master thesis was carried out at ÅF-Industry AB, Helsingborg, during the period from January to May 2014. Supervision has been given by M.Sc. Jimmy Carlsson at ÅF-Industry AB and Associate Professor Håkan Hallberg at Division of Solid Mechanics.

I would like to send a special thanks to my supervisor Jimmy Carlsson for all his guidance and support during this thesis, which has helped me to set up and run analyses in the computational software used and I have received much knowledge about piping systems in general from our discussions. I would also like to thank Håkan Hallberg for his support and feedback during the project.

Further, I want to express my gratitude to all at the Technical Analysis unit in Helsingborg for their engagement and help during the project.

Helsingborg, May 2014
Stefan Alkmyr

Abstract

Several piping systems found in a nuclear power plant are used to transport some fluid under high temperature (e.g. steam). To allow for thermal expansion and avoid excessive thermal stress in these systems, it is necessary to use pipe supports with gaps. Use of this type of support will introduce problems when it comes to analysing the response of the piping system due to time history loading. For this purpose is usually the piping analysis software PIPESTRESS used although it only features linear modelling of pipe supports with gaps in time history analyses. It is known that the results from such an analysis may to some extent include errors due to the linear approximation.

The objectives of this thesis has been to study which influence the modelling of nonlinear pipe supports has when it comes to calculation of maximum reaction forces and moments in the piping system. The parameter study that was carried out on two test models for this purpose showed in general that there were significant differences between the results from the analyses with linear and nonlinear modelling. It was also found that it is difficult to formulate an equation that could be used to approximate the maximum force in a nonlinear support, because gap size and support stiffness are influencing this in different ways depending on which load case that is applied. For one of the used load cases, that excites critical eigenfrequencies in the low frequency range, it was seen that the difference in maximum resultant moment in the piping system between the linear and nonlinear analysis were increasing almost linearly when the gap size was increased, which needs to be accounted for when evaluating stress levels in a piping system.

A typical piping system for emergency core cooling was then analysed with a real time history loading to verify the results from the parameter study. The results showed that the suggested equations (based on the parameter study) gave maximum forces that were rather conservative compared to the corresponding values from the nonlinear analysis for some of the nonlinear supports. Better agreement with the results from the nonlinear analysis was found when using a previously suggested method for approximate calculation of maximum force in a nonlinear support. This was not expected since the parameter study showed significant deviation between the results from the nonlinear analysis and the approximate value calculated with this method for most of the tests. It was also found for some of the nonlinear supports that linear modelling of these actually gives a somewhat higher maximum force than compared with nonlinear modelling.

This thesis has shown that the errors introduced by linear modelling are quite difficult to account for by modifying the result from the linear analysis. Depending on which piping system configuration and load case that are considered, the procedure to correct forces would need to be modified for every combination. Due to this, nonlinear modelling is required to more accurately analyse the response of nonlinear piping systems.

Notations

ΔL	Thermal expansion
M	Bending moment
$h, \Delta t$	Time step
$\boldsymbol{a}, \boldsymbol{u}$	Displacement vector
$\boldsymbol{N}$	Global shape functions
$\boldsymbol{B}$	Gradient of the global shape functions

Other notations used are explained when presented in the report.

Abbreviations

ASME	American Society of Mechanical Engineers
CFD	Computational Fluid Dynamics
CAE	Computer Aided Engineering
BPVC	Boiler and Pressure Vessel Code
FEM	Finite Element Method

Table of Contents

1. Introduction

1.1 Presentation of ÅF

ÅF is a leading technical consulting company with more than a century of experience in the business. The company has approximately 7 000 employees and consists of four divisions: International, Industry, Infrastructure and Technology. ÅF is primarily focusing on offering consultant services in the areas energy, infrastructure (installations, sound and vibrations and infrastructure planning) and industry (e.g. automation, electrical power systems and mechanical engineering). Most of ÅF's costumers and business are located in Europe but are also found in other parts of the world.

The first Swedish steam generator association (named "Södra Sveriges Ångpanneförening") was founded in 1895 by owners of steam generators and pressure vessels. The intention was to perform inspections of pressurised components to help prevent industrial accidents. Two years later "Mellersta och Norra Sveriges Ångpanneförening" was started and the inspectors were now also providing consulting work. It was not until 1964 that the two companies merged into "Ångpanneföreningen", ÅF.

1.2 Background to the project

From a mechanical engineering point of view, a fundamental requirement when designing piping systems and pressure vessels for the nuclear power industry is to secure structural and pressure integrity so that the plant is able to operate safely during various conditions and loads. Rules and guidelines for how to design and evaluate that the pressure carrying components meet the requirements are found in detail in ASME Boiler and Pressure Vessel code III and are also regulated by Swedish national laws.

When verifying that a piping system is fulfilling the requirements set by the ASME code, both static and dynamic analyses are carried out with the help of finite element based piping analysis software. Examples of typical dynamic loads encountered when dealing with piping analyses are water hammers and earthquakes.

The two most common CAE software used to analyse piping systems for the nuclear industry in Sweden are PIPESTRESS and ANSYS. The main advantages with using PIPESTRESS compared with ANSYS are for example built in code evaluation according to ASME, load applications and combinations based on design specifications from the nuclear industry. However, the software also comes with some limitations. One such is that the software only supports linear modelling of pipe supports in time history analyses. In ANSYS one has the possibility to include and model nonlinear pipe supports in this type of analyses.

The error that will be introduced in the solution due to linear approximation of nonlinear pipe supports is not fully known as it may depend on different parameters. It is the scope of this project to investigate how different parameters are influencing this error and if it is possible to establish some kind of rule to compensate for nonlinear effects in piping systems when PIPESTRESS is used for the time history analysis.

1.3 Objectives

This thesis aims at finding an equation that calculates the maximum force in a nonlinear support based on results from a time history analysis with linear modelling of this support. The following steps will be carried out for this purpose:

1. Short literature study of the subject nonlinear piping systems.
2. Learn how ANSYS can be used to model and analyse piping systems with both linear and nonlinear supports.
3. Perform a parameter study in ANSYS on two nonlinear test piping systems with time history loading. The parameters that will be included in the study are gap size, support stiffness, amplitude and frequency content of the time history load.
4. Try to suggest an equation that accounts for nonlinear effects when calculating the maximum force in nonlinear supports that have been approximated as linear in the analysis.
5. Analyse a typical piping system for emergency core cooling to verify the proposed equation.

1.4 Limitations

It was decided that it is of most interest to investigate the behaviour of a nonlinear piping system exposed to water hammer loading. No other dynamic loads such as earthquake will be considered for this reason. Further, no thermal effects will be considered in this project. When it comes to modelling of the piping material a limitation has been made to only use a linear material model. Finally the piping analyses will only be performed with the finite element software ANSYS (version 14.5). The reason for this is that both linear and nonlinear supports can be used in time history analyses in ANSYS while PIPESTRESS is limited to linear modelling of supports.

2. ASME Boiler and Pressure Vessel code Section III

The ASME Boiler and Pressure Vessel code Section III is used when verifying that the design of a piping system is fulfilling certain requirements for use in the nuclear industry. The piping systems found in a nuclear power plant are divided into three different safety classes in this code:

- Class 1 - Piping systems that are within the nuclear reactor coolant pressure boundary.
- Class 2 - Piping systems that are important to the plant safety (e.g. emergency core cooling)
- Class 3 - Piping systems that are found in the cooling water and auxiliary feedwater systems.

The BPVC specifies an allowable stress level for the piping system based on which service level (A-D) that are considered. Choice of service level should be based on what type of loads that the piping system should be evaluated for. The different service levels are described in section 2.1 and in [1].

2.1 Service levels

2.1.1 Level A

Loads that the piping system may be subjected to during normal operating conditions are referred to as level A loadings in the BPVC code. Level A usually consists of loads due to operating pressure and weight (so called sustained loads).

2.1.2 Level B

Level B loadings are defined as those occasional loads[1] that the piping system must sustain without suffering damage requiring repair. Water hammer, relief valve discharge and operating basis earthquake[2] are examples of loads that are included in level B.

2.1.3 Level C

Loads due to postulated design accidents of the plant are classified as level C loadings. If the plant would be exposed to level C loadings, it is a requirement that the safety functions of the piping systems must be working as designed to ensure safe shutdown. Before starting up the plant after a level C event, inspections and any repairs of piping components are carried out although damage is not expected. One example of a level C loading is safe shutdown earthquake which is defined as the maximum earthquake assumed to occur at the plant site at any time.

2.1.4 Level D

The most critical loads are included in level D. These loads are due to worst case scenarios such as loss of coolant accidents and earthquakes with very high magnitude. Higher stress levels in the piping system are allowed for level D but the requirement is still that the safety functions must be able to perform as expected.

[1] Loads that the piping system are exposed to only during a small fraction of the total operating time.
[2] Defined as the maximum earthquake that is assumed to occur within the design lifetime of the plant or one half of the safe shutdown earthquake, depending on which is greater.

2.2 Subsection NC and ND

To conclude this section, the two equations (found in subsection NC and ND in BPVC and in [1]) that are used to evaluate a class 2 or 3 piping system due to sustained or occasional loading are presented. The requirement stated in the equations must be met in all nodal points to conclude that the piping system is properly design for a specific loading condition.

$$S_{SL} = \frac{B_1 P D_o}{2t_n} + \frac{B_2 M_A}{Z} \leq 1.5 S_h \tag{2.1}$$

$$S_{OL} = \frac{B_1 P_{max} D_o}{2t_n} + \frac{B_2 (M_A + M_B)}{Z} \leq n S_h \tag{2.2}$$

where

B_1, B_2	Primary stress indices for the evaluated component
P	Internal design pressure
P_{max}	Peak pressure
D_o	Outer diameter of pipe
t_n	Nominal wall thickness
M_A	Resultant moment loading due to sustained loads
M_B	Resultant moment loading due to occasional loads
Z	Section modulus of pipe
S_h	Material allowable stress at design temperature
n	Load-level-dependent factor (e.g. $n = 1.8$ if load level B)

3. Piping systems

Piping systems are used in nuclear power plants and other applications as well to transport liquids or gases between various components. Depending on the application the complexity of the piping system may vary from a small number of interconnected pipes with only a few components to a very large number of pipes including many in-line components (e.g. valves, flanges and t-connections) and other components like pumps, heat exchangers and tanks.

3.1 Supports

Supports are needed in piping systems to carry the weight of the entire system including the transported fluid and any insulation. Besides the weight load the supports must also be capable of transferring any other load on the structure that may occur during operation.

When determining which type of pipe supports that should be used and where to place them in the piping system to achieve a design that fulfils all load requirements, trade-offs usually have to be made. To explain this, consider first dynamic loads such as earthquakes and water hammers. These loads are best resisted by use of rigid supports that restrains the displacements in the piping system, to avoid excessive bending and torsional moments and impacts between pipes and supports. Consider next thermal expansion loads that will be present in piping systems that transfers fluids under high temperature. To allow for the thermal expansion given by equation (3.1), it is necessary to use spring supports or supports with gaps that introduce some flexibility to the piping system. Use of rigid supports would in this case cause problems with excessive thermal stress.

$$\Delta L = \alpha \Delta T L_0 \tag{3.1}$$

where

α Thermal expansion coefficient
ΔT Temperature difference
L_0 Original length (or outer diameter) of pipe

The types of pipe supports that will be used in this project are briefly explained in the following sections and for a more detailed description of various pipe supports the reader is referred to [1].

3.1.1 Spring support

Spring support, as the name suggests, consists of a spring that is attached between a supporting structure and the pipe. Because springs can resist both tension and compression loads they are suitable to use for supporting weight and thermal expansion loads. A special variant of spring support is the so called constant force support which includes a mechanism that provides a uniform force irrespective of the deformation.

3.1.2 Guide support

The guide support shown in figure 3.1 is built as a frame of I-beams that is installed around the pipe with some gap. This ensures that the main movement of the pipe will be in the direction parallel to its centreline while some thermal expansion in the other directions will not be restricted by the support.

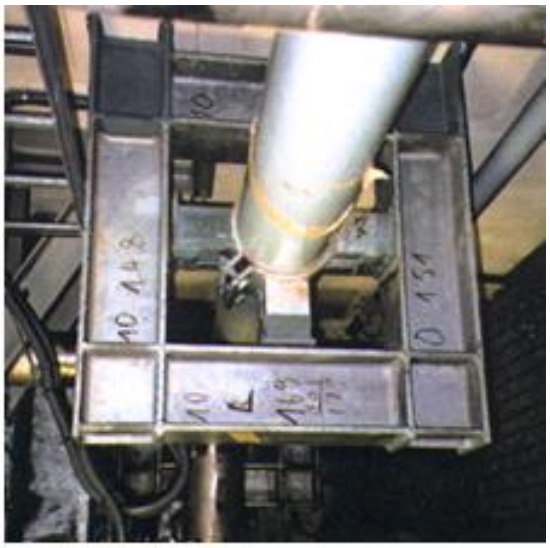

Figure 3.1: Example of a guide support in a piping system.

3.1.3 One-way support

This support type can be considered as a guide support with infinite gap in the directions perpendicular and opposite to the support direction, as shown in figure 3.2. One-way supports cannot resist lift loads due to the fact that the pipe is not attached in some way to the support. This means that if the loading condition in the piping system is such that a force acting in the opposite direction to the gravitational field becomes larger than the weight load, the pipe will be able to lift from the support.

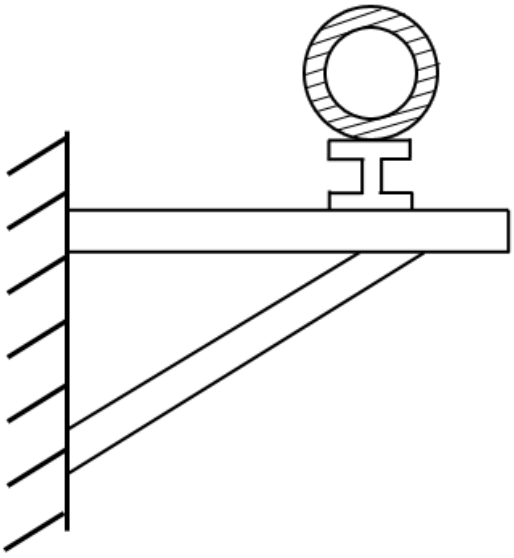

Figure 3.2: Illustration of a one-way support.

3.1.4 Anchor

Anchor is a type of rigid support that restrains movement in all degrees of freedom (three translational and three rotational) and is possible to use where there is no significant thermal expansion in the piping system.

3.2 Difference between linear and nonlinear supports

Pipe supports may in general be divided into two groups having either linear or nonlinear stiffness, where the constant force support makes an exception. With linear/nonlinear stiffness one means that the support force varies in either a linear or nonlinear way with the support deformation. For clarity some different plots illustrating the difference are presented in figure 3.3 to 3.6. In figure 3.3, a one-way support is shown to have stiffness only in the support direction. If a lift stop is added to this support the result will be stiffness in the other direction as well (after the gap is closed) which can be seen in figure 3.4. The stiffness plot shown in figure 3.5 represents a spring support, where the stiffness is seen to vary in a linear way irrespective of whether the support is loaded in tension or compression. Note that if the spring support would for some reason reach maximum compression due to the loading situation, the slope of the curve will increase and result in stiffness as shown in figure 3.6.

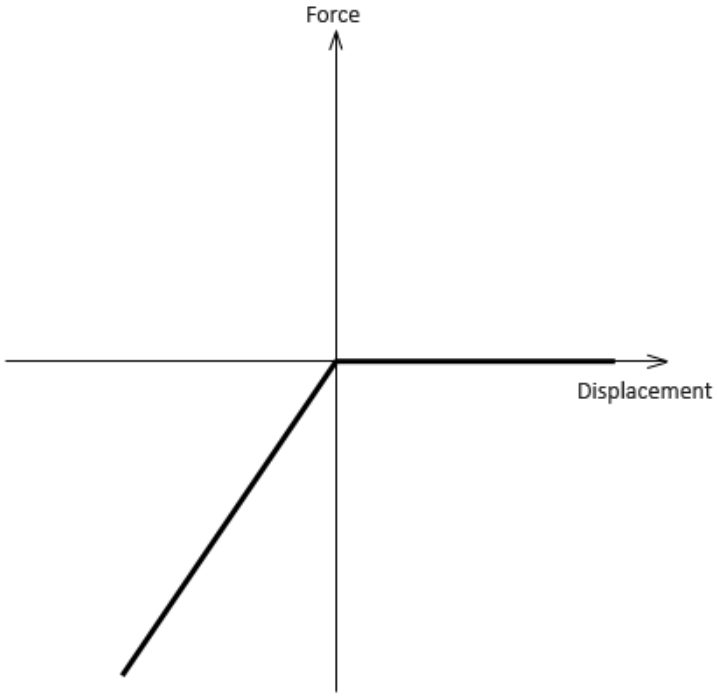

Figure 3.3: Force vs. displacement for a one-way support.

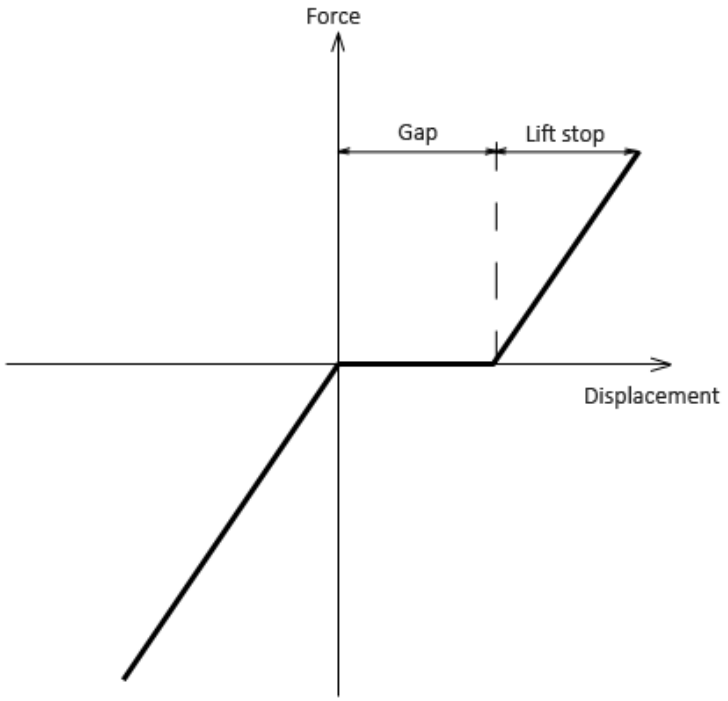

Figure 3.4: Force vs. displacement for a one-way support with lift stop.

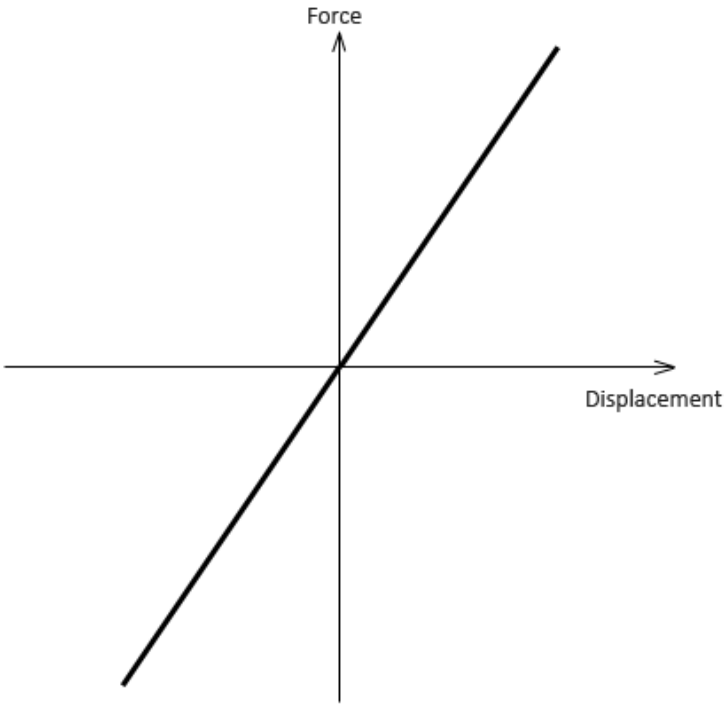

Figure 3.5: Stiffness characteristics for a spring support.

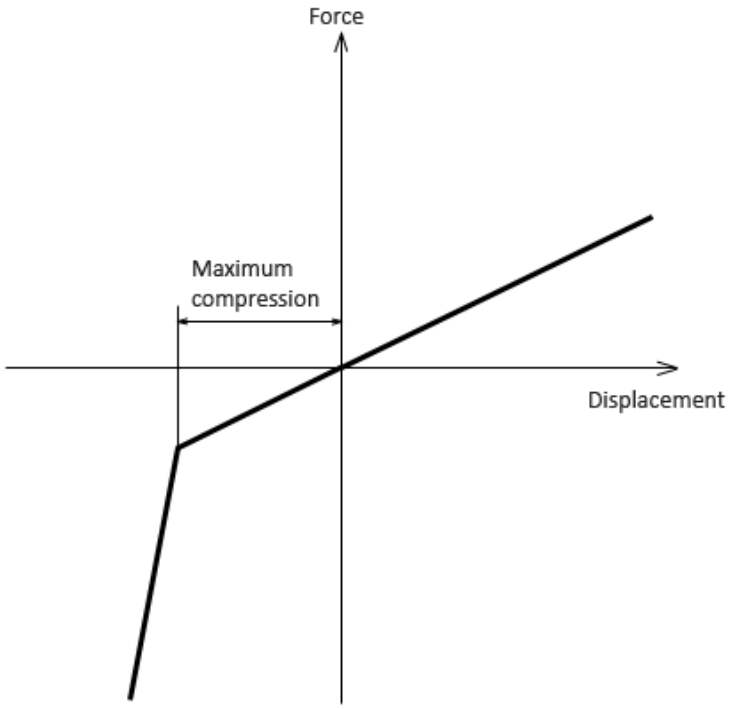

Figure 3.6: Shows the change in stiffness when a spring support reaches maximum compression.

4. Water hammer

One of the loads that a piping system must be designed to sustain is a water hammer. This type of load occurs when there is a sudden change in operating conditions or flow direction that causes pressure variations in the piping system due to unsteady water flow. As described in [2] the main events that trigger water hammers are:

- Power failure
- Starting or stopping pumps
- Opening or closing shut-off valves

The reason for water hammer loads to occur in piping systems is that when increasing/decreasing the flow velocity, a variation in pressure must follow to provide the necessary force for acceleration or retardation. Depending on how fast the rate of change in flow velocity is and the size of it, the magnitude of the corresponding change in pressure will vary. For the most critical cases when either the pressure rise or pressure fall becomes large enough, a pressure wave will be initiated in the piping system. This will then propagate back and forth through the system until the energy has dissipated due to friction and impacts between pipes and supports. As a consequence of the initiated pressure wave, vibrations and a characteristic hammering noise will appear in the piping system. Vibrations could eventually cause significant damage to piping systems if resonant frequencies are excited and the system is not properly supported.

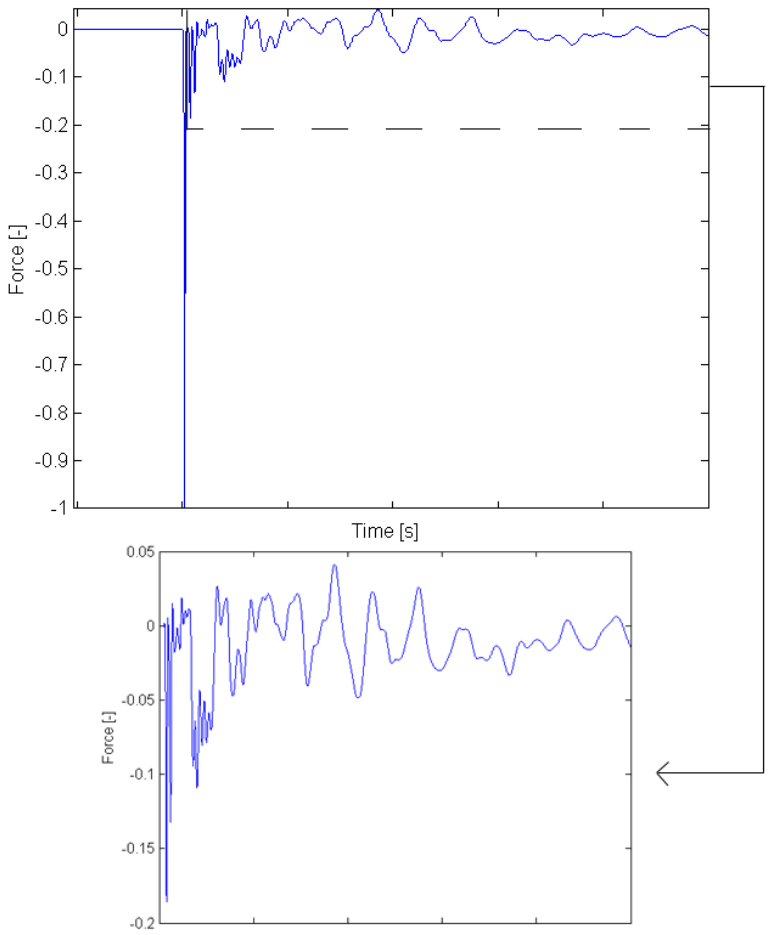

Figure 4.1: Example of a water hammer load.

Water hammer loads in nuclear piping systems are usually determined by use of specialised one-dimensional fluid flow solvers like RELAP5 or multi-dimensional CFD codes. Figure 4.1 illustrates an example of a water hammer load at some point in a piping system (note that the load is presented with normalised values).

5. Introduction to the Finite Element Method

The finite element method is often used for the numerical simulations of piping systems. The basis of this numerical method is summarised in this section. In the FEM the approach is to discretise the geometry into a finite number of elements as shown in figure 5.1. By doing this and introducing an approximation of how the solution variable (e.g. temperature, concentration and displacement) varies in the elements, it is possible to reformulate the governing equation of the problem into a set of equations that gives the exact solution to the problem at the nodal points. One could then use the finite element approximations to calculate an approximate solution in other parts of the geometry.

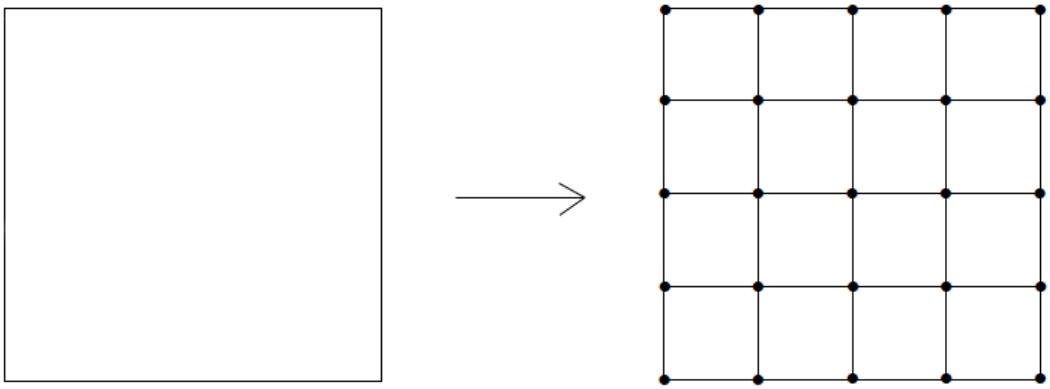

Figure 5.1: The discretised geometry (i.e. the mesh) is shown to the right where the plate has been divided into elements.

The main steps involved when deriving a finite element formulation will be summarised below for a simple beam problem to illustrate the method. For more details the reader is referred to [3]. Consider the beam shown in figure 5.2 with a constant cross-sectional area A and the loading $q(x)$ (unit [N/m]).

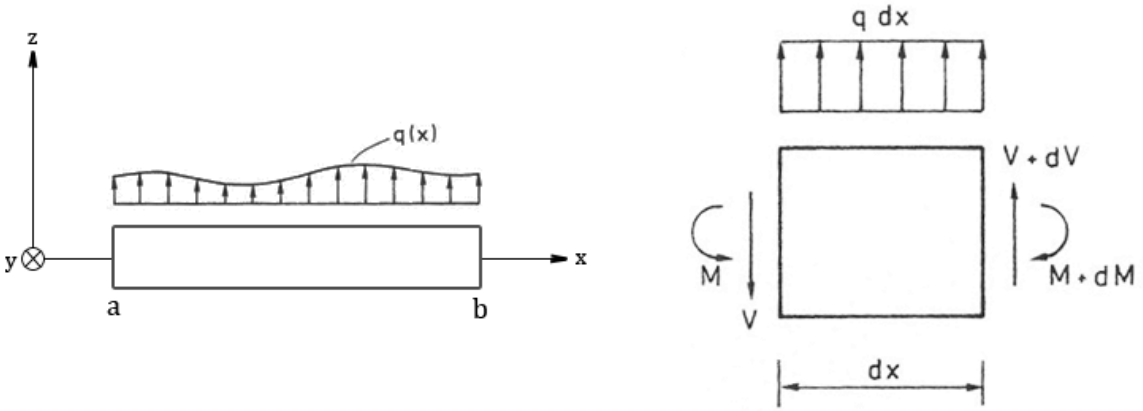

Figure 5.2: Shows the forces and moments acting on an infinitesimal small part of a beam.

The two equilibrium equations for this problem are given by

$$\frac{dM}{dx} = V, \qquad \frac{dV}{dx} = -q \tag{5.1}$$

By elimination of the shear force V, the strong form of the problem is obtained

$$\frac{d^2M}{dx^2} + q = 0 \tag{5.2}$$

(5.2) is then multiplied with an arbitrary weight function v and integrated over the beam, which gives the following equation

$$\int_a^b v\frac{d^2M}{dx^2}dx + \int_a^b vqdx = 0 \tag{5.3}$$

Use of integration by parts on the first term in (5.3) yields

$$[vV]_a^b - \int_a^b \frac{dv}{dx}\frac{dM}{dx}dx + \int_a^b vqdx = 0 \tag{5.4}$$

Use of integration by parts once more on the second term in (5.4) gives

$$[vV]_a^b - \left[\frac{dv}{dx}M\right]_a^b + \int_a^b \frac{d^2v}{dx^2}Mdx + \int_a^b vqdx = 0 \tag{5.5}$$

Insertion of the FE approximation and the choice of weight function in (5.6)

$$w = \boldsymbol{N}\boldsymbol{a}, \quad \frac{d^2w}{dx^2} = \boldsymbol{B}\boldsymbol{a}, \quad v = \boldsymbol{N}\boldsymbol{c}, \quad \frac{dv}{dx} = \frac{d\boldsymbol{N}}{dx}\boldsymbol{c}, \quad \frac{d^2v}{dx^2} = \boldsymbol{B}\boldsymbol{c} \tag{5.6}$$

into (5.5) and noticing that the vector $\boldsymbol{c}$ is arbitrary, the weak form of the problem is obtained

$$\int_a^b \boldsymbol{B}^T EI\boldsymbol{B}dx\boldsymbol{a} = [\boldsymbol{N}^T V]_a^b - \left[\frac{d\boldsymbol{N}^T}{dx}M\right]_a^b - \int_a^b \boldsymbol{N}^T qdx \tag{5.7}$$

where the relation

$$M = -EI\frac{d^2w}{dx^2} = -EI\boldsymbol{B}\boldsymbol{a} \tag{5.8}$$

has been used to arrive at the expression in (5.7).

Finally (5.7) can now be written in the compact format in (5.9) which represents the FE formulation of the problem

$$\boldsymbol{K}\boldsymbol{a} = \boldsymbol{f} \tag{5.9}$$

where the stiffness matrix $\boldsymbol{K}$ and force vector $\boldsymbol{f}$ are defined as

$$\boldsymbol{K} = \int_a^b \boldsymbol{B}^T EI\boldsymbol{B}dx, \quad \boldsymbol{f} = [\boldsymbol{N}^T V]_a^b - \left[\frac{d\boldsymbol{N}^T}{dx}M\right]_a^b - \int_a^b \boldsymbol{N}^T q dx \tag{5.10}$$

One may note that all terms in the expression for the force vector in (5.10) should be evaluated at (or integrated between) the two end points of the beam. In order to calculate the force vector so called natural boundary conditions (because they appear naturally when deriving the FE formulation) are needed which in this case would be values of the shear force and bending moment in node a or b. Usually the beam is fixed in one end which means that the deflection is zero ($w = 0$) but the moment and shear force is unknown. This type of boundary condition is called an essential boundary condition. A sufficient number of natural and essential (or mixed) boundary conditions are required to get a solution to the problem.

6. Time history analysis

To determine the response of a piping system due to time history loading the equations of motion in (6.1) can be solved by using either direct time integration or the mode superposition method.

$$\boldsymbol{M\ddot{u}} + \boldsymbol{C\dot{u}} + \boldsymbol{Ku} = \boldsymbol{f}(t) \tag{6.1}$$

In this equation $\boldsymbol{M}$ is the mass matrix, $\boldsymbol{C}$ represents the damping matrix, $\boldsymbol{u}$ is the displacement vector and the force vector $\boldsymbol{f}$ is now a function of time. A superposed dot denotes differentiation with respect to time and hence are $\dot{\boldsymbol{u}}$ and $\ddot{\boldsymbol{u}}$ the velocity and acceleration vector.

PIPESTRESS uses the mode superposition method to solve (6.1). As described in [4] the idea in this method is to transform the equations of motion into a set of n uncoupled equations (where n is the number of eigenfrequencies and mode shapes) by expressing the displacements in terms of generalised displacements. Then only the equations with the frequencies that are excited by the dynamic loads need to be solved to get an approximate solution to the response of the structure. This shortens the computational time required for the analysis but the transformation is only valid for linear problems. That is the reason why PIPESTRESS only accepts linear modelling of supports when performing time history analysis.

When analysing nonlinear piping systems in ANSYS another method called direct time integration will be used instead. This method solves the equations of motion at different time steps by use of some numerical time stepping technique. The Newmark algorithm will be applied in this project for the integration of (6.1). A description of this algorithm is given in the section 6.1 and follows that presented in [5].

6.1 Newmark algorithm

The Newmark algorithm is an integration procedure that starts from time step n at time t_n where the displacement and velocity vector $(\boldsymbol{u}_n, \dot{\boldsymbol{u}}_n)$ are assumed to be known and also the force vectors $\boldsymbol{f}_n$ from the current time and $\boldsymbol{f}_{n+1}$ from the next time step $n+1$ at time $t_{n+1} = t_n + h$. By integration of $\boldsymbol{u}$ and $\dot{\boldsymbol{u}}$ from t_n to t_{n+1} the following expressions for the displacement and velocity vector $(\boldsymbol{u}_{n+1}, \dot{\boldsymbol{u}}_{n+1})$ can be formulated

$$\boldsymbol{u}_{n+1} = \boldsymbol{u}_n + \int_{t_n}^{t_{n+1}} \dot{\boldsymbol{u}}(\tau) d\tau \tag{6.2}$$

$$\dot{\boldsymbol{u}}_{n+1} = \dot{\boldsymbol{u}}_n + \int_{t_n}^{t_{n+1}} \ddot{\boldsymbol{u}}(\tau) d\tau \tag{6.3}$$

Comparing these two equations shows that (6.3) integrates the accelerations $\ddot{\boldsymbol{u}}$ while (6.2) integrates the velocity $\dot{\boldsymbol{u}}$. Due to this, (6.2) must be rewritten such that it includes $\ddot{\boldsymbol{u}}$ instead. To achieve this, $\dot{\boldsymbol{u}}$ is first multiplied by a factor of 1

$$\boldsymbol{u}_{n+1} = \boldsymbol{u}_n + \int_{t_n}^{t_{n+1}} 1 * \dot{\boldsymbol{u}}(\tau) d\tau \tag{6.4}$$

It is now possible to use integration by parts on the second term on the right side of equation (6.4). In [5] the integral of the factor 1 is selected as $\tau - t_{n+1}$which gives (6.5) and further (6.6)

$$\boldsymbol{u}_{n+1} = \boldsymbol{u}_n + [(\tau - t_{n+1})\dot{\boldsymbol{u}}(\tau)]_{t_n}^{t_{n+1}} + \int_{t_n}^{t_{n+1}} (t_{n+1} - \tau)\ddot{\boldsymbol{u}}(\tau)d\tau \tag{6.5}$$

$$\boldsymbol{u}_{n+1} = \boldsymbol{u}_n + h\dot{\boldsymbol{u}}_n + \int_{t_n}^{t_{n+1}} (t_{n+1} - \tau)\ddot{\boldsymbol{u}}(\tau)d\tau \tag{6.6}$$

The problem now is that it will not be known how the accelerations are varying between t_n and t_{n+1}. To deal with this the integrals in (6.3) and (6.6) are approximately calculated as a weighted sum of $\ddot{\boldsymbol{u}}_n$ and $\ddot{\boldsymbol{u}}_{n+1}$ according to

$$\begin{aligned} \int_{t_n}^{t_{n+1}} \ddot{\boldsymbol{u}}(\tau)d\tau &\approx (1-\gamma)h\ddot{\boldsymbol{u}}_n + \gamma h\ddot{\boldsymbol{u}}_{n+1} \\ \int_{t_n}^{t_{n+1}} (t_{n+1} - \tau)\ddot{\boldsymbol{u}}(\tau)d\tau &\approx \left(\frac{1}{2} - \beta\right)h^2\ddot{\boldsymbol{u}}_n + \beta h^2\ddot{\boldsymbol{u}}_{n+1} \end{aligned} \tag{6.7}$$

Insertion of (6.7) in (6.3) and (6.6) gives the equations in (6.8) which calculate the displacements and velocities at the next time step. Note that the only unknown variables in these equations are the accelerations at time t_{n+1}.

$$\begin{aligned} \boldsymbol{u}_{n+1} &= \boldsymbol{u}_n + h\dot{\boldsymbol{u}}_n + \left(\frac{1}{2} - \beta\right)h^2\ddot{\boldsymbol{u}}_n + \beta h^2\ddot{\boldsymbol{u}}_{n+1} \\ \dot{\boldsymbol{u}}_{n+1} &= \dot{\boldsymbol{u}}_n + (1-\gamma)h\ddot{\boldsymbol{u}}_n + \gamma h\ddot{\boldsymbol{u}}_{n+1} \end{aligned} \tag{6.8}$$

Combining (6.1) and (6.8) yields an expression (6.9) that makes it possible to calculate $\ddot{\boldsymbol{u}}_{n+1}$. Substitution into (6.8) then gives the displacements $\boldsymbol{u}_{n+1}$ and velocities $\dot{\boldsymbol{u}}_{n+1}$.

$$(\boldsymbol{M} + \gamma h\boldsymbol{C} + \beta h^2\boldsymbol{K})\ddot{\boldsymbol{u}}_{n+1} = \boldsymbol{f}_{n+1} - \boldsymbol{C}(\dot{\boldsymbol{u}}_n + (1-\gamma)h\ddot{\boldsymbol{u}}_n) - \boldsymbol{K}\left(\boldsymbol{u}_n + h\dot{\boldsymbol{u}}_n + \left(\frac{1}{2} - \beta\right)h^2\ddot{\boldsymbol{u}}_n\right) \tag{6.9}$$

The Newmark algorithm is summarised below. One may note that the algorithm is based on a prediction-correction procedure where the displacements and velocities for the next time step are first approximately calculated. (6.9) is then solved to get the new accelerations. These are then used to correct the predicted values.

The Newmark time integration algorithm

(1) Compute the modified mass matrix $\boldsymbol{M}_*$ from

$$\boldsymbol{M}_* = \boldsymbol{M} + \gamma h \boldsymbol{C} + \beta h^2 \boldsymbol{K}$$

(2) Calculate initial accelerations $\ddot{\boldsymbol{u}}_0$ based on the initial conditions $\boldsymbol{u}_0, \dot{\boldsymbol{u}}_0$

$$\ddot{\boldsymbol{u}}_0 = \boldsymbol{M}^{-1}(\boldsymbol{f}_0 - \boldsymbol{C}\dot{\boldsymbol{u}}_0 - \boldsymbol{K}\boldsymbol{u}_0)$$

(3) Predict values for $\boldsymbol{u}_{n+1}, \dot{\boldsymbol{u}}_{n+1}$

$$\dot{\boldsymbol{u}}^*_{n+1} = \dot{\boldsymbol{u}}_n + (1-\gamma)h\ddot{\boldsymbol{u}}_n$$

$$\boldsymbol{u}^*_{n+1} = \boldsymbol{u}_n + h\dot{\boldsymbol{u}}_n + \left(\frac{1}{2} - \beta\right)h^2\ddot{\boldsymbol{u}}_n$$

(4) Calculate accelerations $\ddot{\boldsymbol{u}}_{n+1}$ by solving (6.9)

$$\ddot{\boldsymbol{u}}_{n+1} = \boldsymbol{M}_*^{-1}(\boldsymbol{f}_{n+1} - \boldsymbol{C}\dot{\boldsymbol{u}}^*_{n+1} - \boldsymbol{K}\boldsymbol{u}^*_{n+1})$$

(5) Correct the predicted values $\boldsymbol{u}^*_{n+1}, \dot{\boldsymbol{u}}^*_{n+1}$

$$\dot{\boldsymbol{u}}_{n+1} = \dot{\boldsymbol{u}}^*_{n+1} + \gamma h\ddot{\boldsymbol{u}}_{n+1}$$

$$\boldsymbol{u}_{n+1} = \boldsymbol{u}^*_{n+1} + \beta h^2\ddot{\boldsymbol{u}}_n$$

(6) If $t_{n+1} > t_{end}$ then quit, else return to (3) for new time step

Depending on which values that are chosen for the Newmark parameters β and γ the solution will be either unconditionally stable or unstable. If chosen as presented in (6.10) the solution will be unconditionally stable

$$\gamma \geq \frac{1}{2}, \qquad \beta \geq \frac{1}{2}\gamma \tag{6.10}$$

In this project $\gamma = \frac{1}{2}$ and $\beta = \frac{1}{4}$ will be used to avoid introducing artificial numerical damping into the solution.

6.2 Rayleigh damping

The damping matrix in equation (6.1) is often assumed to be a linear combination of the mass and stiffness matrix, which is referred to as Rayleigh damping

$$\boldsymbol{C} = \alpha \boldsymbol{M} + \beta \boldsymbol{K} \tag{6.11}$$

It is possible to derive the expression in (6.12) for the critical damping ratio of the i:th mode ξ_i which includes the α and β parameters and the circular eigenfrequency of the i:th mode ω_i

$$\xi_i = \frac{\alpha}{2\omega_i} + \frac{\beta \omega_i}{2} \tag{6.12}$$

Assume now that the critical damping ratio is approximately constant over a frequency interval $[\omega_1, \omega_2]$. Use of equation (6.12) now gives two equations where α and β can be solved for

$$\alpha = 2\xi \frac{\omega_1 \omega_2}{\omega_1 + \omega_2}, \qquad \beta = \frac{2\xi}{\omega_1 + \omega_2} \tag{6.13}$$

An example of how the critical damping ratio varies with the frequency when Rayleigh damping is applied can be seen in figure 6.1. From the figure, it is seen that the α-damping determines the damping in the low frequency part while β-damping influence the damping in the high frequency part.

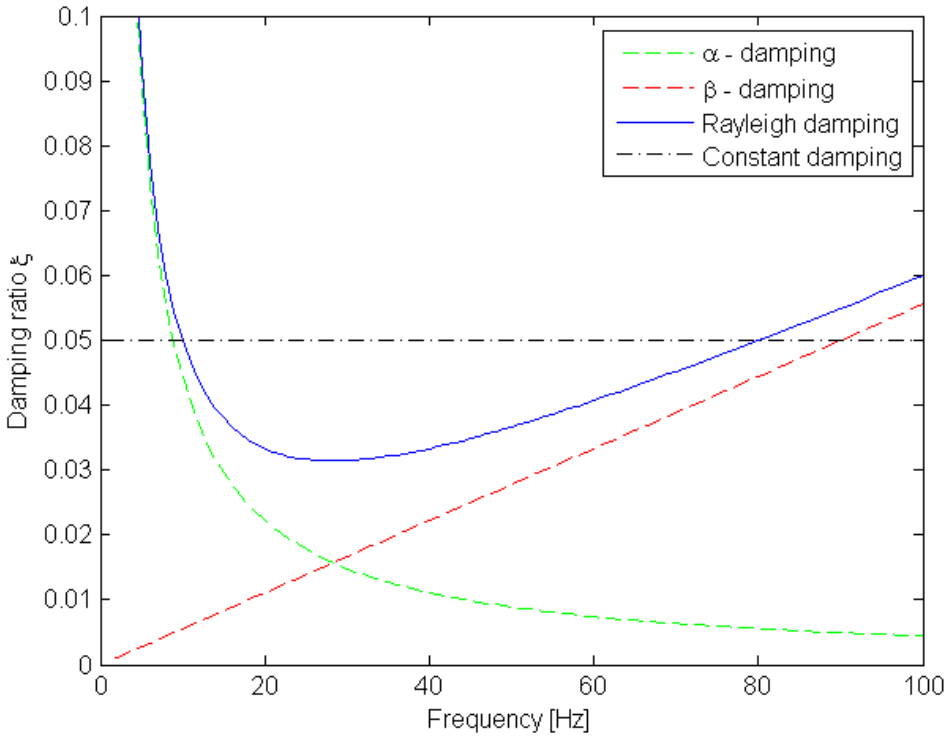

Figure 6.1: Rayleigh damping for the case with $\omega_1 = 20\pi$, $\omega_2 = 160\pi$ and $\xi = 0.05$.

The approach when determining the frequency interval to use for the Rayleigh damping will follow that described in [6]. The lower bound of the frequency interval $\omega_1$should then be based on the first eigenfrequency of the piping system while the upper bound ω_2 will be set equal to the highest frequency of the applied water hammer load.

6.3 Time step

One of the parameters that are of importance in time history analyses is the time step. To get an accurate solution, the time step should be set to an appropriate value that captures the response of the piping system due to the highest frequency contained in the load. A suitable value to use when the Newmark time stepping technique is used is given in [6] and in (6.14)

$$\Delta t \leq \frac{2\pi}{10\omega_c} \tag{6.14}$$

where

ω_c Cut off frequency [rad/s]

6.4 Element length

When discussing the influence of the time step in the previous section, it could be observed from (6.14) that the higher the cut off frequency the lower the time step needs to be chosen. This may lead to very time consuming analyses if a nonlinear piping system with high frequency loading should be simulated for instance. To be able to capture the response of the piping system without having to use a very small time step, one could change the size of the element length instead. An analytical relation between the bending wavelength λ and the natural frequency ω has been derived for a slender beam and is given in [6]. Based on this relation it is then suggested in [6] that an acceptable element length may be determined from the expression in (6.15)

$$L_{element} \leq \frac{\lambda(\omega_c)}{6} = \frac{\pi}{6\sqrt{\omega_c}}\left(\frac{8r^2E}{\rho_{tot}}\right)^{\frac{1}{4}}, \qquad \rho_{tot} = \rho_{pipe} + \frac{\rho_{medium}\pi(r - t/2)^2 + m_{insulation}}{2\pi rt} \tag{6.15}$$

where

$L_{element}$	Maximum acceptable element length
$r = r_o - t/2$	Middle radius of pipe material (r_o - outer radius)
E	Young's modulus
t	Pipe wall thickness
ρ_{pipe}	Density of pipe material
ρ_{medium}	Density of medium in the pipe
$m_{insulation}$	Mass of insulation per unit length

7. Modelling of piping systems in ANSYS

7.1 Pipes

In the parameter study that will be performed in this project, it is of main interest to study how reaction forces and moments vary when nonlinearities in the piping system are included in the analysis or approximated as linear. For that purpose the most simple and practical way of modelling the pipes in the system is by using pipe elements which basically are 3-D beam elements with modified element stiffness and mass matrix due to the pipe cross section. These pipe elements has one node at each end and a total of six degrees of freedom at each node, namely three translations u_x, u_y and u_z and three rotations φ_x, φ_y and φ_z (see figure 7.1).

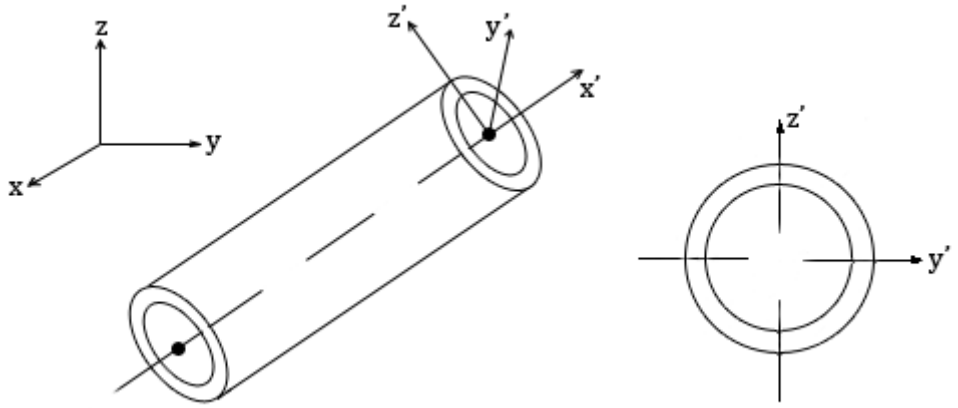

Figure 7.1: Pipe element (note that x, y, z is the global coordinate system while x', y', z' is the element coordinate system).

ANSYS comes with a piping module that includes the linear elastic pipe elements PIPE16 and PIPE18 and the current technology pipe elements PIPE288 and ELBOW290. The main difference between these elements is that the latter are based on Timoshenko beam theory while the first is using Euler-Bernoulli beam theory instead [7]. Timoshenko beam theory takes shear deformations into account [8] which better describes the behaviour of pipes with a low ratio between length and wall thickness. These effects are neglected in Euler-Bernoulli beam theory and holds as a good assumption for long slender pipes with a high ratio between length and wall thickness. In general piping analysis performed with elements based on Euler-Bernoulli beam theory are considered to give acceptable results according to [6] and also longer simulation times would probably be required with the updated elements. For these reasons the older pipe elements will be used for the analyses in the parameter study.

7.2 Piping components

Piping components such as valves, reducers and t-connections may be modelled in ANSYS by using PIPE16 elements with additional specifications (e.g. weight and stress intensification factors).

7.3 Pipe supports

7.3.1 Linear

Linear supports are modelled in ANSYS by connecting the spring element COMBIN14 [7] directly to the pipe. To model anchor in the same way in ANSYS as in PIPESTRESS, three translational and rotational springs will be added in the global coordinate directions to the node where the anchor is to be placed (instead of constraining all degrees of freedom in the anchor node).

7.3.2 Nonlinear

To model the nonlinear supports in ANSYS, a node-node contact element CONTA178 [7] connected in series with a spring element COMBIN14 will be used (same approach as in [9]). With this configuration the purpose of the contact element is to activate/deactivate the spring support depending on whether the gap is open or closed. The way of modelling the linear/nonlinear supports are schematically presented in figure 7.2.

It was found from analyses, where the contact algorithm was chosen as either the Lagrange multiplier method or the Penalty method, that the first gave the most accurate modelling of nonlinear supports. For the case with the Lagrange multiplier method the calculated lift force in the one-way support was zero (when the maximum allowable tensile contact force FTOL [7] was set to a small value, e.g. 1 N) while the results from the analysis with the Penalty method showed a non-zero value. Because a one-way support cannot sustain any lift force, it is clear that the Lagrange multiplier method is a better choice of contact algorithm in this case.

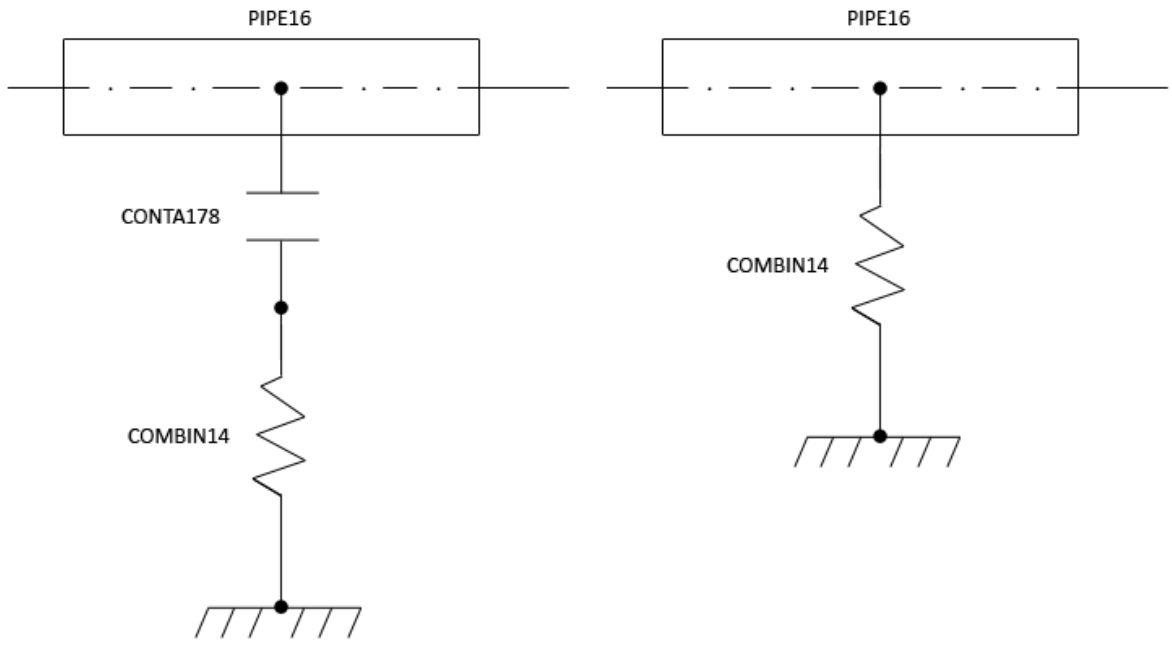

Figure 7.2: Nonlinear modelling (to the left) and linear modelling (to the right) of pipe supports in ANSYS.

It should be mentioned that effects of friction between the pipe and guide or one-way support will be neglected in this project. The reason is that influence of friction in piping systems has already been studied to some extent in [9] and it was concluded that neglecting the effect of friction gives conservative results.

8. Parameter study

8.1 Test models

The ANSYS models of the two nonlinear test piping systems that will be used for the analyses in the parameter study are shown in figure 8.1 and 8.2. As can be seen in figure 8.1 and 8.2, the piping models consist of both straight and curved pipes with dimensions in the range from DN25 up to DN300 (which corresponds to an outer diameter between 33.4 and 324 mm and wall thickness between 4.46 and 17.45 mm). The test models also contain typical piping components like valves, reducers, flanges and t-connections.

8.2 Materials

The piping systems are made out of two types of steel materials with properties according to table 8.1 that are valid at a temperature of 21℃. Pipes with dimensions above DN50 and all supports are assigned the steel material number 1 and steel material number 2 is used for pipes with lower dimensions than (or equal to) DN50.

Table 8.1: Properties for the two piping materials.

Material number	Young's modulus [GPa]	Poisson's ratio [-]	Density [kg/m^3]
1	177	0.3	8100
2	190	0.3	8100

8.3 Supports

The piping models contain both linear and nonlinear supports, whose orientation (presented in direction cosines) and stiffness can be found in table 8.2. From table 8.2 it can be noted that the guide support (support number 1) is modelled differently in the two test models. For test model 1 the guide support will be nonlinear with a 2 mm gap in both the x-direction and positive y-direction between the pipe clamp and the supporting frame. With no gap in the negative y-direction the support resembles a one-way support with lift stop and constraints in the tangential direction. The guide support will be modelled as linear in test model 2 to only include one nonlinearity in the system.

In addition to the supports listed in table 8.2, an anchor is placed at the end of the pipe run where support number 1, 2 and 4 are positioned. At the other ends of the piping system, all degrees of freedom will be constrained ($u_x = u_y = u_z = \varphi_x = \varphi_y = \varphi_z = 0$) which together with the constraints in the ending node of the supports ($u_x = u_y = u_z = 0$) sets boundary conditions for the models.

Table 8.2: The supports used in the two test models.

Support number and type	Modelling	Support orientation			Stiffness
		x	y	z	
1. Guide support	Nonlinear/ Linear*	1	1	0	50 kN/mm
2. One-way support	Nonlinear	0	1	0	50 kN/mm
3. Spring support	Linear	0	1	0	0.01 kN/mm
3. Torsional spring support	Linear	0.707	0	0.707	$1.13*10^{12}$ kN*mm/rad
4. Spring support	Linear	0	1	0	50 kN/mm
5. Spring support	Linear	0	1	0	100 kN/mm
6. Constant force support	Linear	0	1	0	-

* Modelled as nonlinear in test model 1 and linear in test model 2.

Prestress are applied to some of the spring supports in the piping system according to table 8.3. One way of modelling the prestress in ANSYS is by placing a point load in the node where the pipe is connected to the spring support (see the red arrows in figure 8.1 and 8.2).

Table 8.3: Applied prestress force in some of the supports.

Support number	Prestress force [N]
3	8300
4	200
6	9610

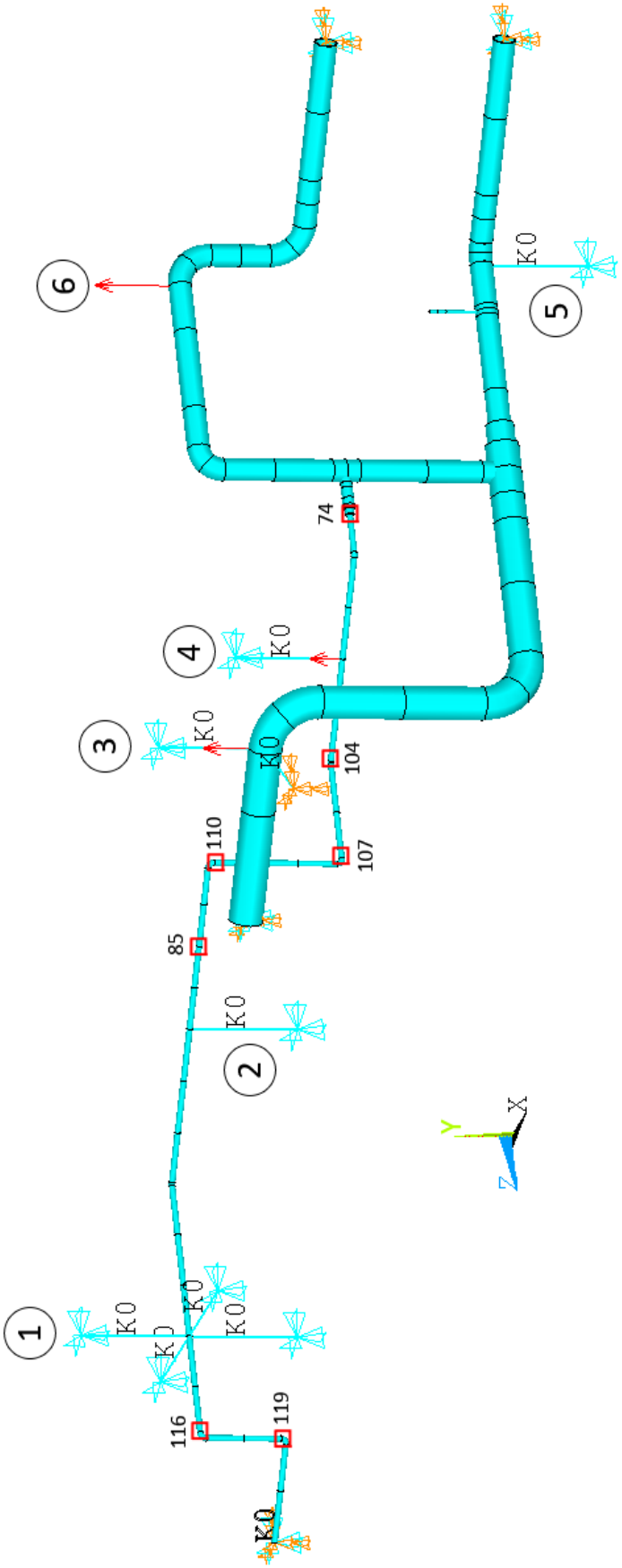

Figure 8.1: Test model 1 (load application nodal points marked with a red box).

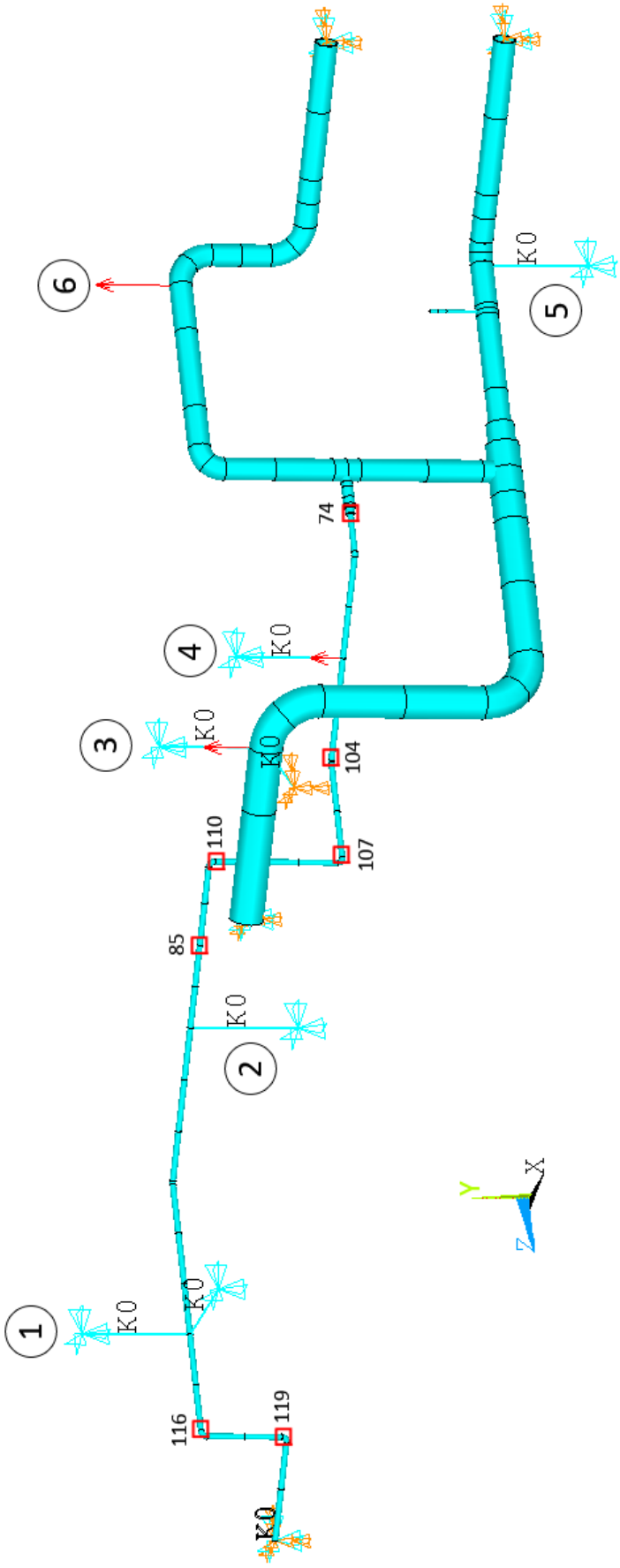

Figure 8.2: Test model 2 (load application nodal points marked with a red box).

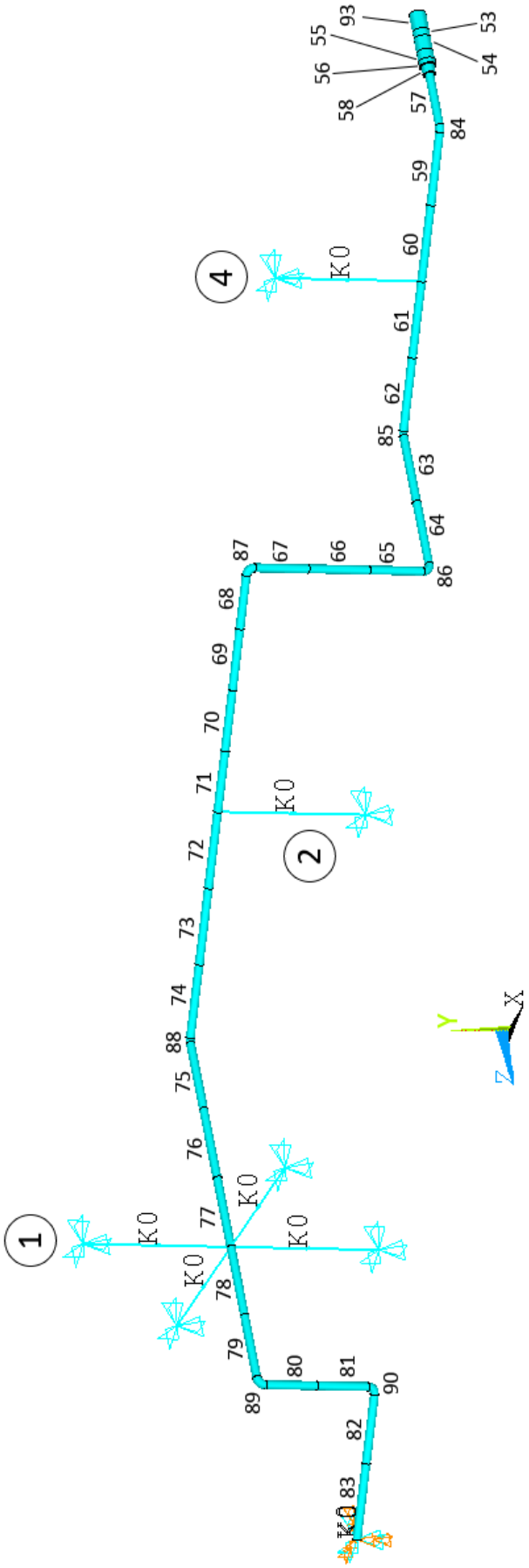

Figure 8.3: Shows the numbers of the elements at the pipe run containing support number 1, 2 and 4.

8.4 Loads

The loads applied to the piping model are dead weight[3], internal pressure and water hammer. Internal pressure is set to 3.8 MPa in all pipes with a DN value larger than 50 and 1.8 MPa in the rest of the system. The water hammer load is simplified to a damped sinus shaped load given by the equation (8.1)

$$f(t) = Ae^{-kt} \sin \omega t \tag{8.1}$$

where

A Amplitude
k Constant (set to 2.8)
ω Angular frequency
t Time

To include the influence of the frequency content of the water hammer load in the parameter study, three load cases with the same amplitude but different frequency content will be used in the analyses. The purpose of the first two load cases is to excite the most critical eigenfrequencies in the lower and higher frequency range, while the third covers frequencies that are non-critical for comparison. Critical eigenfrequencies means in this case eigenfrequencies where the corresponding mode shapes indicate that the nodal points, in which the water hammer load acts, will oscillate much.

The three load cases can be seen in sections 8.4.1 to 8.4.3 and the frequency content for each load case is presented in appendix A.2. In figure 8.1 and 8.2, the nodal points at which the water hammer is applied are marked.

[3] Total weight of the piping system including pipes, external insulation, internal fluid and other in-line components

8.4.1 Load case 1

The nodal loads that are applied in load case 1 are shown in figure 8.4 to 8.6.

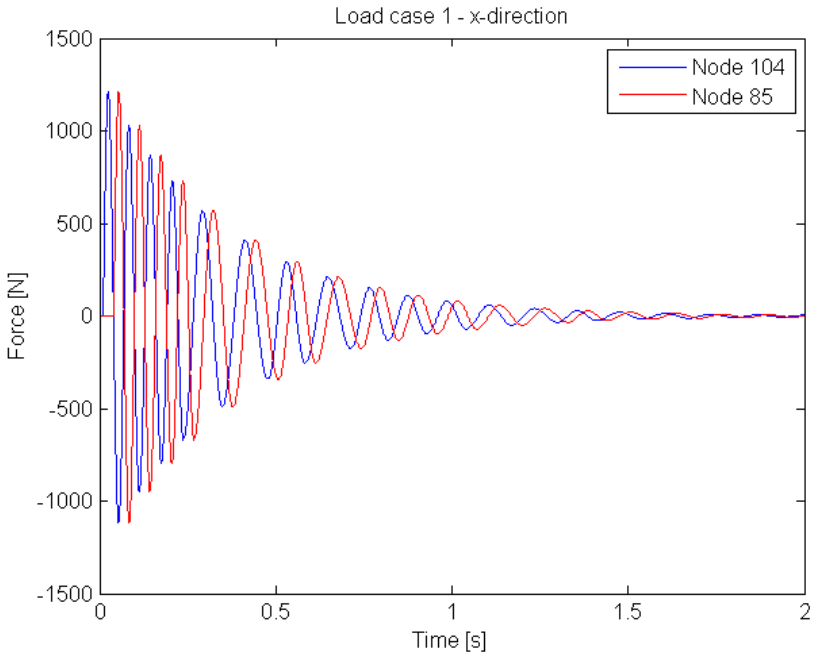

Figure 8.4: Nodal loads applied in x-direction for the first water hammer load case.

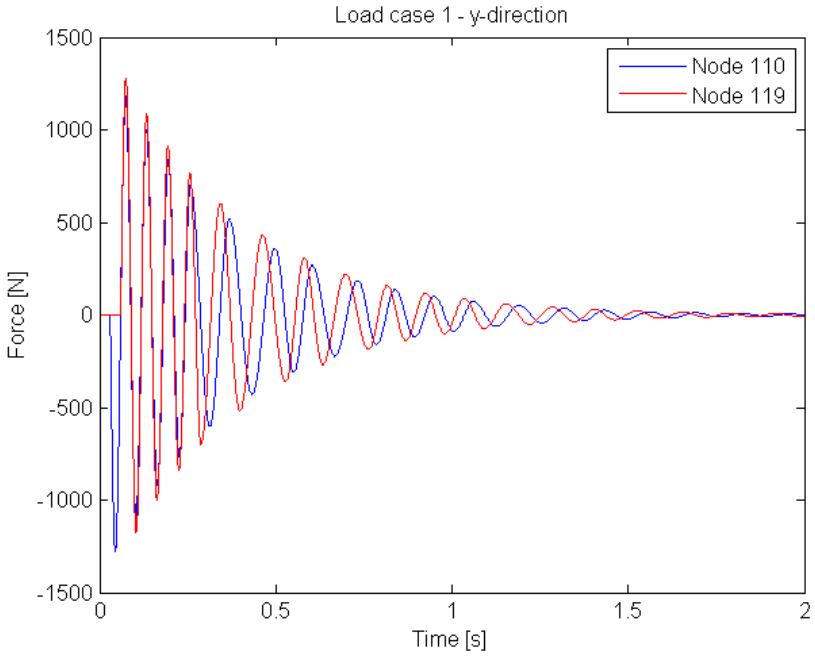

Figure 8.5: Nodal loads applied in y-direction for the first water hammer load case.

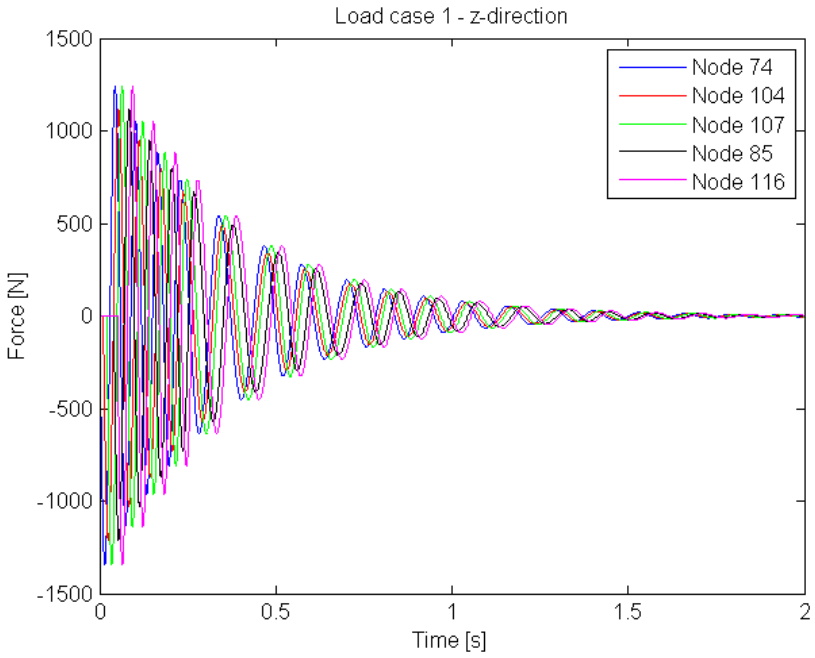

Figure 8.6: Nodal loads applied in z-direction for the first water hammer load case.

8.4.2 Load case 2

The nodal loads that are applied in load case 2 are shown in figure 8.7 to 8.9.

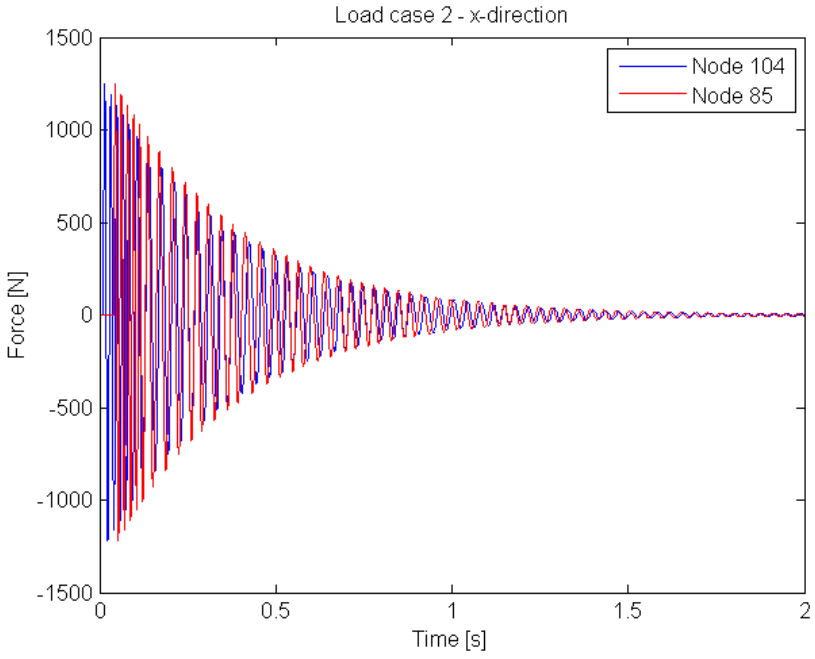

Figure 8.7: Nodal loads applied in x-direction for the second water hammer load case.

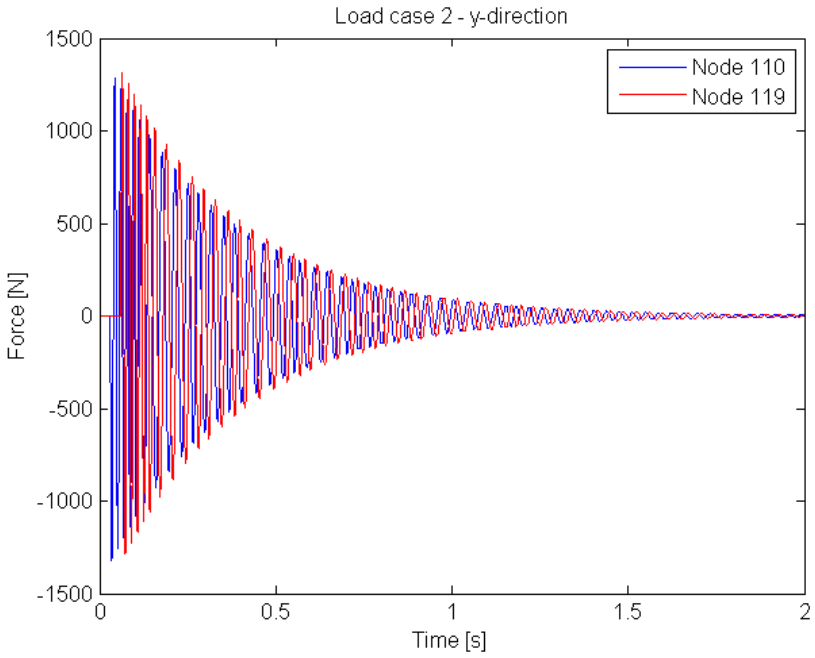

Figure 8.8: Nodal loads applied in y-direction for the second water hammer load case.

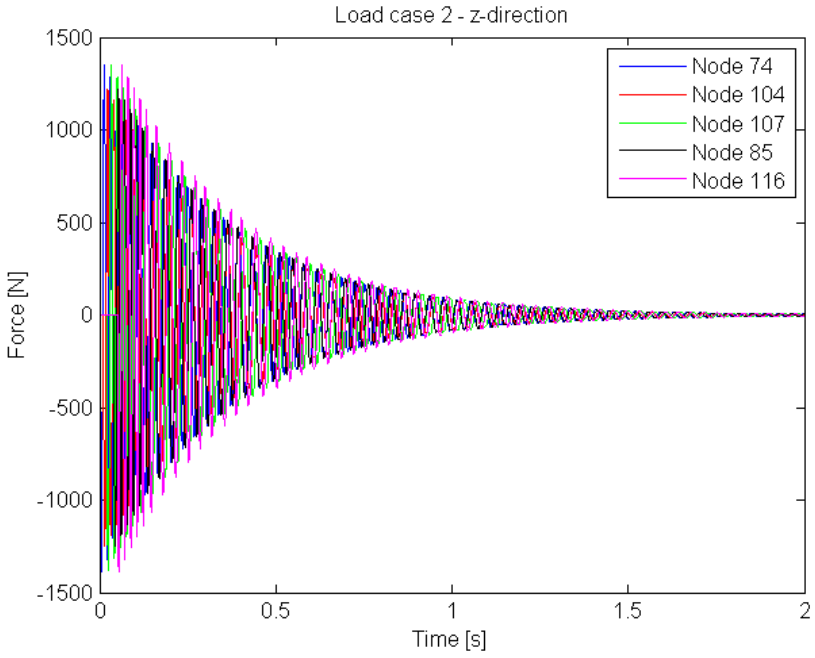

Figure 8.9: Nodal loads applied in z-direction for the second water hammer load case.

8.4.3 Load case 3

The nodal loads that are applied in load case 3 are shown in figure 8.10 to 8.12.

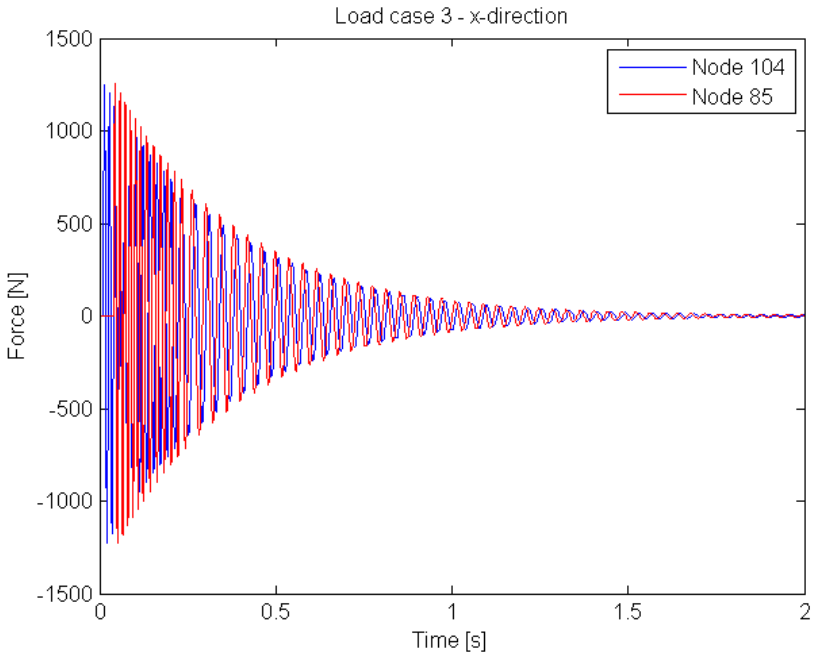

Figure 8.10: Nodal loads applied in x-direction for the third water hammer load case.

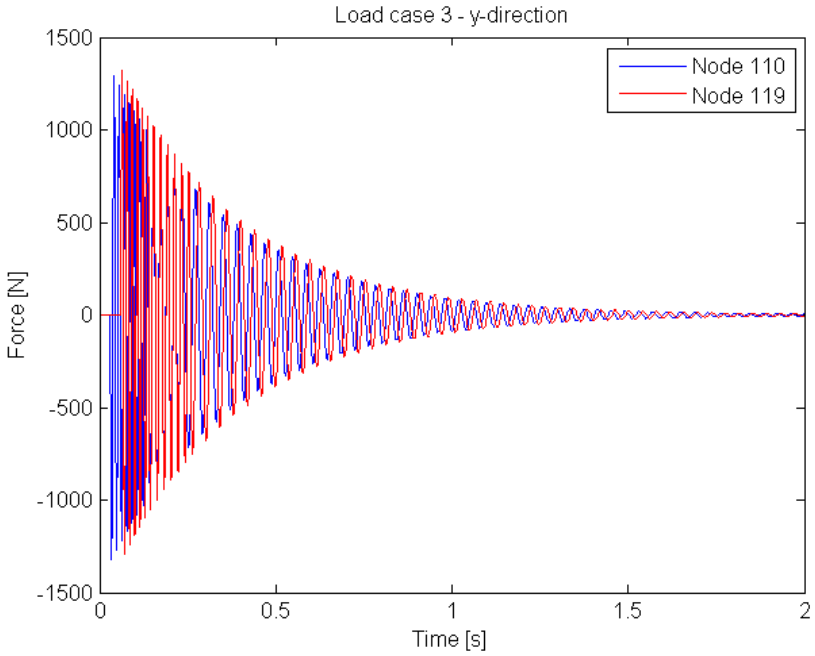

Figure 8.11: Nodal loads applied in y-direction for the third water hammer load case.

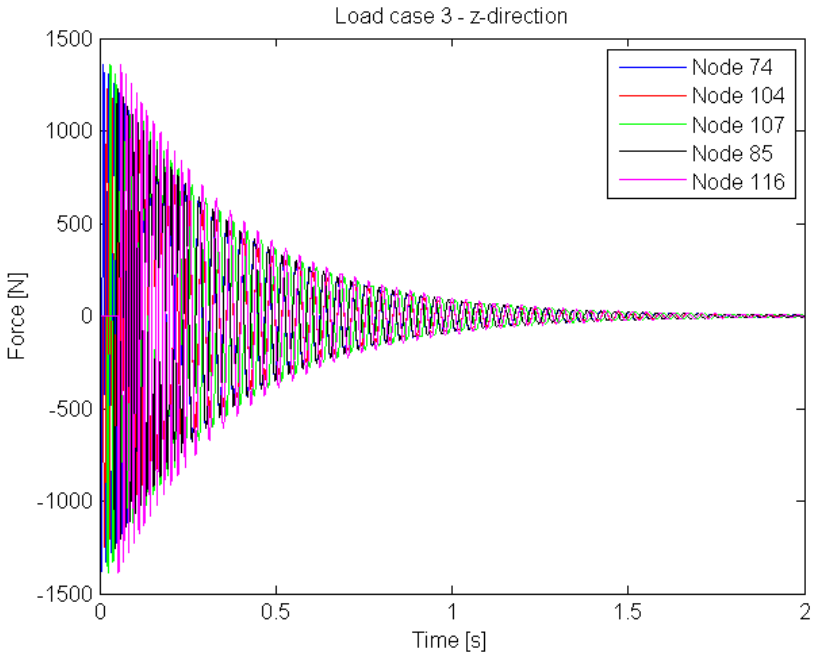

Figure 8.12: Nodal loads applied in z-direction for the third water hammer load case.

8.5 Analyses

The following parameters will be included in the study and are varied as follows:

- *Amplitude of the applied water hammer load*
  The amplitude of the water hammer load (in x, y and z-direction) shown in figure 8.4 to 8.12 is varied from -500 N to +500 N in steps of 100 N.

- *Support stiffness*
  The stiffness of support number 1, 2 and 4 will be varied from 30 kN/mm to 120 kN/mm in steps of 10 kN/mm.

- *Gap size*
  The size of the gap in the guide support (both x and y-direction) will be varied from 1 mm to 15 mm in steps of 1 mm.

To every parameter variation will two analyses be carried out, one linear where all supports are modelled as linear (just as in PIPESTRESS) and one nonlinear where nonlinearities (i.e. gaps) are modelled. Then when both types of analyses are performed in the parameter study, the static loads (weight and internal pressure) will first be applied in a load step to give initial conditions for the second load step where the time varying water hammer load is then applied and solved for.

8.6 Typical piping system

The typical piping system that will be used to verify the proposed equation from the parameter study is seen in figure 8.13. This piping system is used for emergency cooling of the reactor in case of an event that causes the normal cooling systems to malfunction. The piping system contains two main pipe runs with dimensions in the range from DN50 up to around DN200 (corresponding to an outer diameter between 60.3 mm and 219.1 mm and a wall thickness between 8.74 mm and 20.6 mm). One may note that several linear (spring supports) and nonlinear supports (one-way) are placed along the pipe runs. A real water hammer load will be applied to the larger pipe run of the typical piping system including the static load in terms of dead weight.

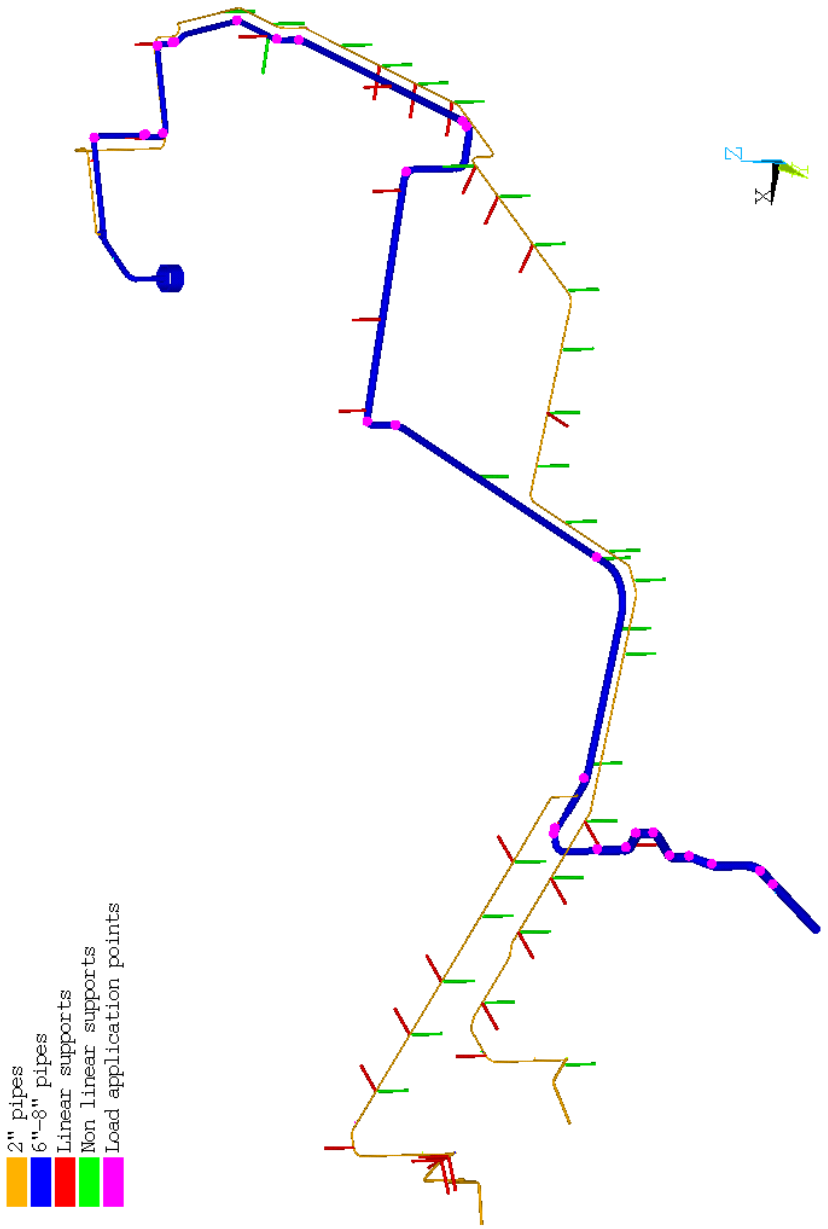

Figure 8.13: ANSYS model of the typical piping system.

9. Results

9.1 Amplitude of the applied water hammer load

9.1.1 Guide support

Figure 9.1 to 9.3 show the results for support number 1 when test model 1 is used and the amplitude of the applied water hammer load is varied. The blue line in figure 9.1 to 9.3 shows the maximum force in y-direction for the guide support which has been determined from the nonlinear analysis. The red line shows the approximate value for the maximum force when a previously suggested method is used, that is based on results from the linear analysis. This will be referred to as the previous method throughout the rest of the report and is described in detail in appendix A.1. The black line represents the equation that best corresponds to the values from the nonlinear analysis (i.e. the blue line). Finally the green and the pink lines show the maximum lift[4] and compression force in the guide support when modelled as linear.

One may note from the results that the approximate maximum force based on the previous method is not consistent in any of the load cases with the value from the nonlinear analysis. The difference between the two results is most noticeable for the first and second load case with excitation of critical frequencies within the low and high frequency range. Slightly better agreement with the nonlinear results is found for the load case with excitation of non-critical frequencies when the amplitude is increased.

When considering the suggested equations in figure 9.1 to 9.3 that calculates the maximum force based on values from the linear analysis, it becomes clear that it is not possible to use the same choice of factors for the different load cases. For the second and third load case, the maximum lift force term can almost be neglected since the maximum force are not varying that much from a mean value that is determined by the dead weight load multiplied by an amplification factor. This is in contrast to the first load case where the maximum force is seen to increase with increasing amplitude, which requires that the lift force term is included with a quite large amplification factor.

[4] Force due to pipe displacement in the vertical upward direction when a one-way support is modelled as linear.

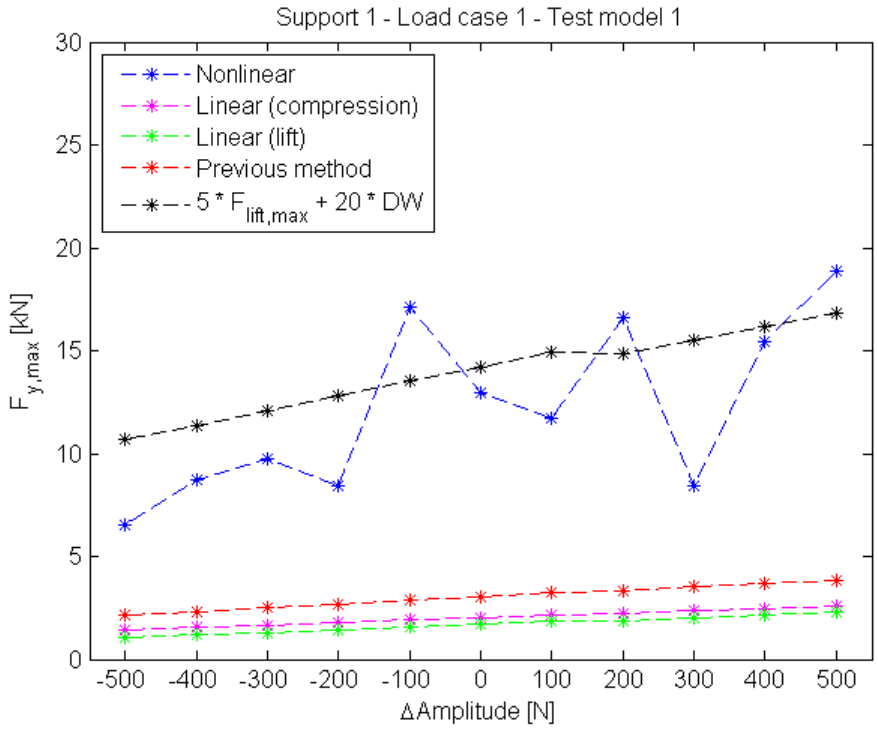

Figure 9.1: Maximum force in support number 1 when the amplitude in load case 1 is varied.

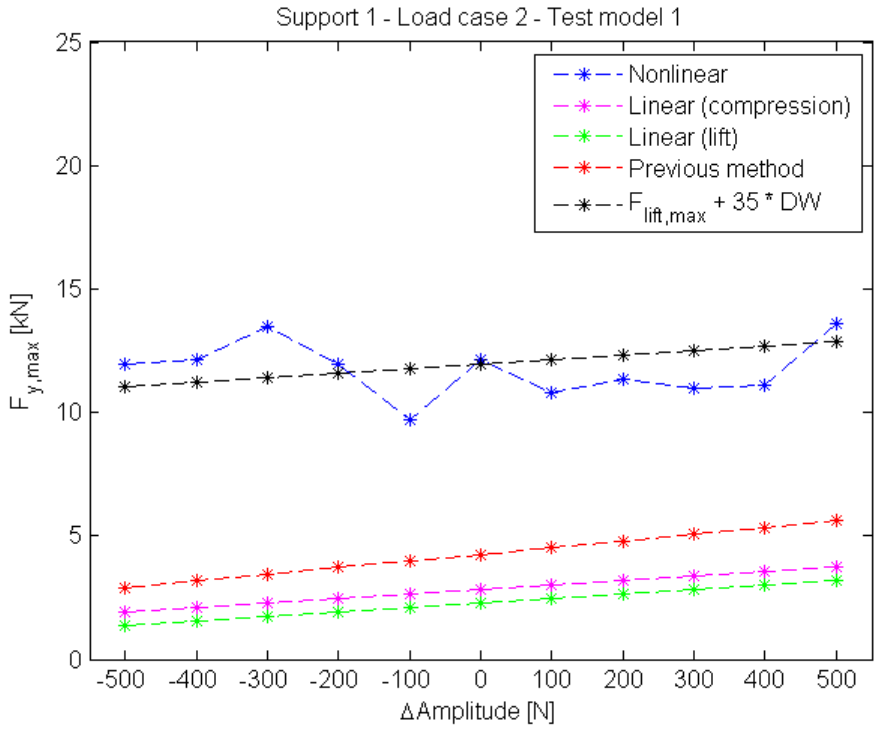

Figure 9.2: Maximum force in support number 1 when the amplitude in load case 2 is varied.

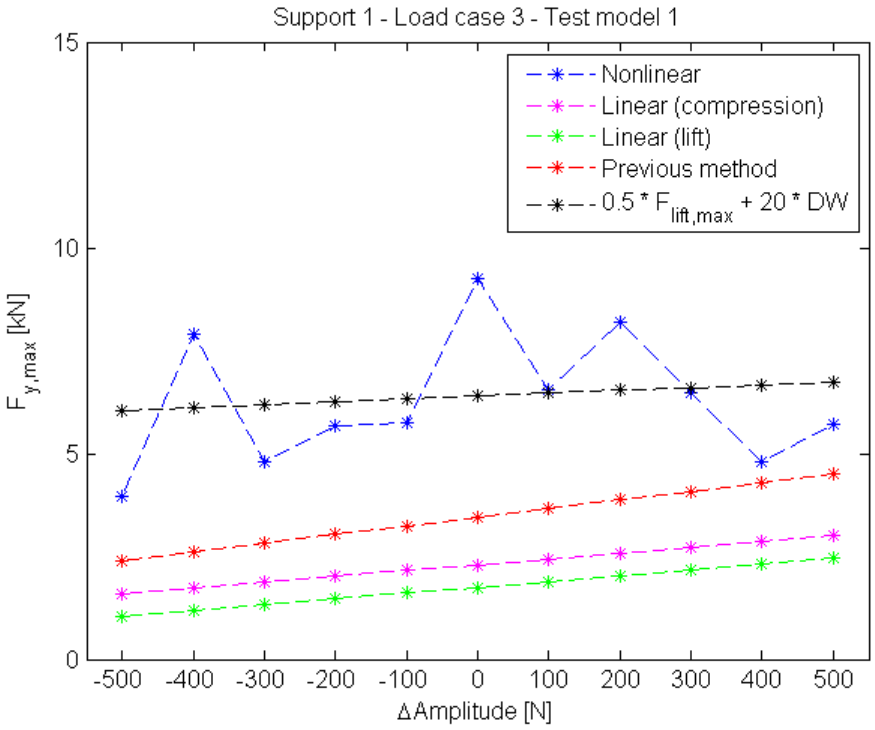

Figure 9.3: Maximum force in support number 1 when the amplitude in load case 3 is varied.

9.1.2 One-way support

In figure 9.4 to 9.9 are the results presented for support number 2 when the two test models are used and the three water hammer load cases are applied respectively. According to the results, use of the previous method will only give a good approximation of the maximum force when the amplitude of the water hammer load is decreased from its original value, i.e. when the maximum lift and compression force is lowered.

The maximum force determined from the nonlinear analysis is seen to increase almost linearly as the amplitude is increasing for the case with both linear and nonlinear modelling of the guide support. One may note that use of test model 2 gives higher contact forces than compared to test model 1. This is seen to result in that the maximum lift force must be multiplied with different factors depending on which configuration of piping system and load case that is considered.

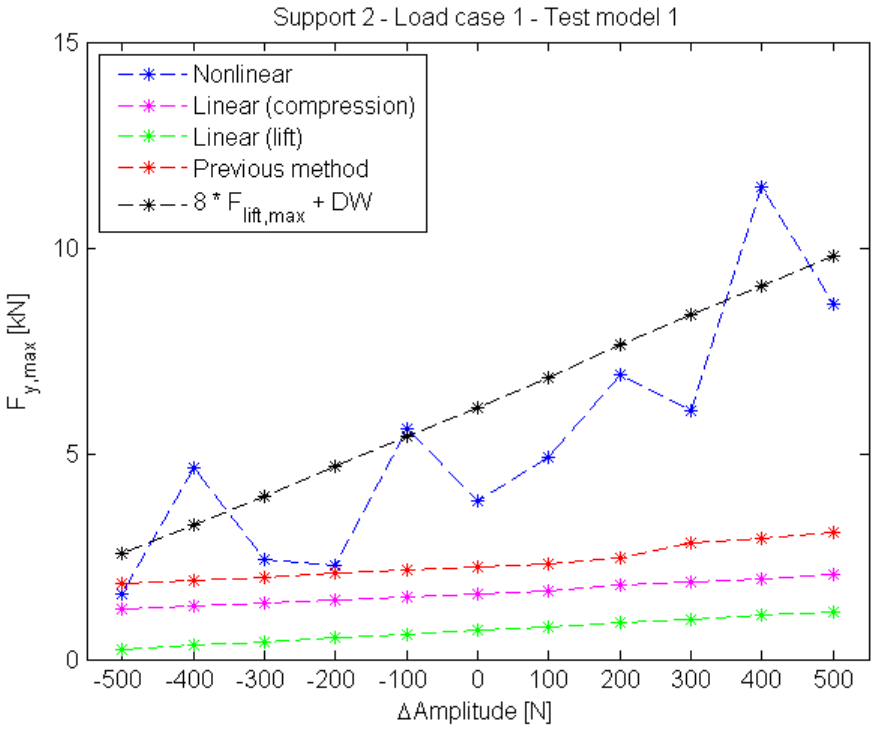

Figure 9.4: Maximum force vs. change of amplitude in load case 1 for support number 2 (test model 1).

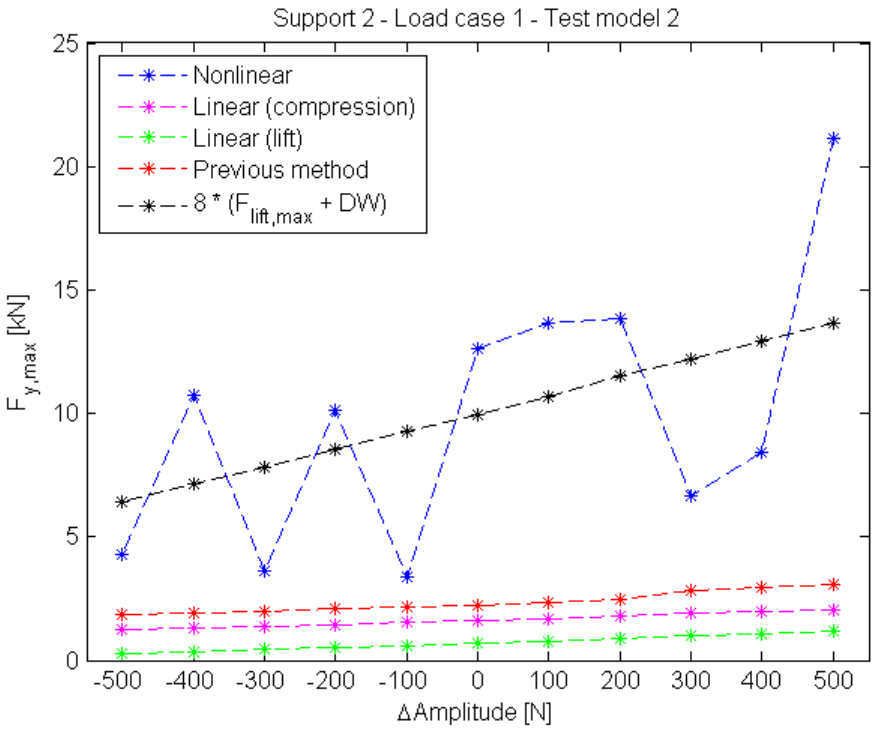

Figure 9.5: Maximum force vs. change of amplitude in load case 1 for support number 2 (test model 2).

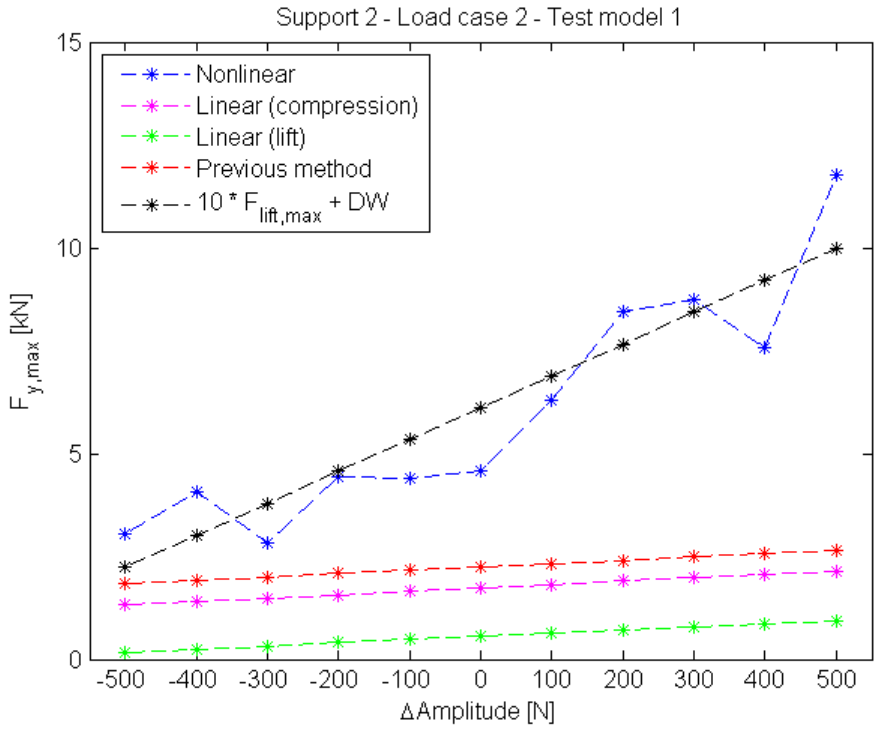

Figure 9.6: Maximum force vs. change of amplitude in load case 2 for support number 2 (test model 1).

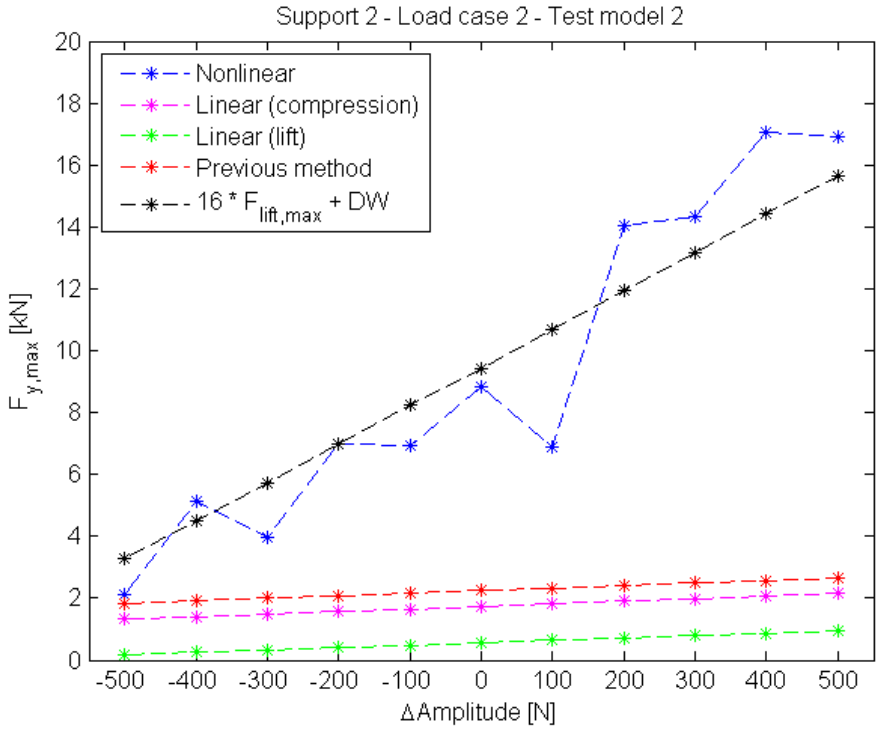

Figure 9.7: Maximum force vs. change of amplitude in load case 2 for support number 2 (test model 2).

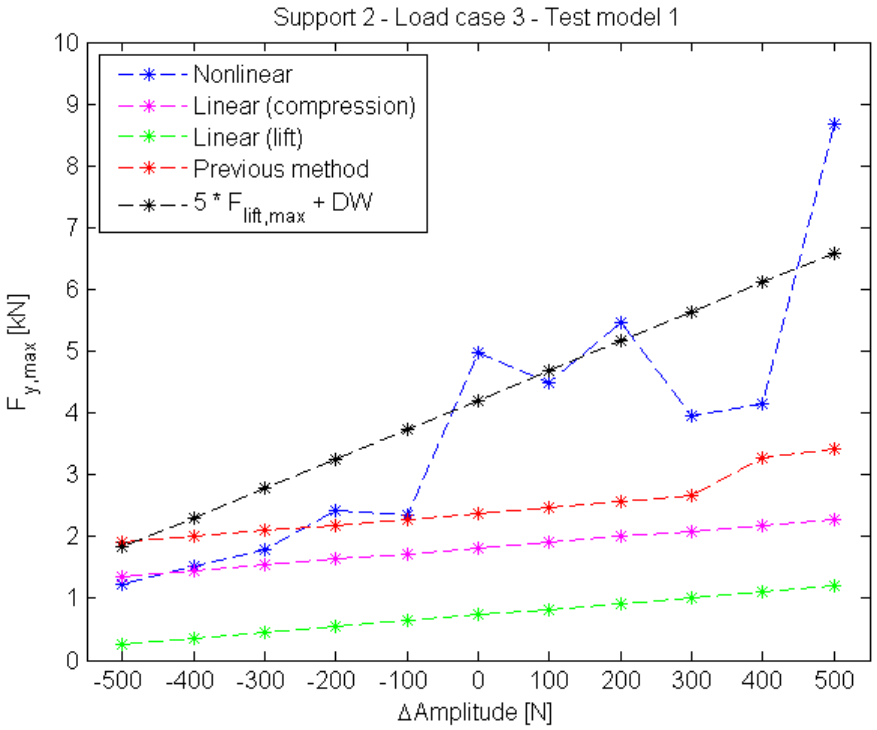

Figure 9.8: Maximum force vs. change of amplitude in load case 3 for support number 2 (test model 1).

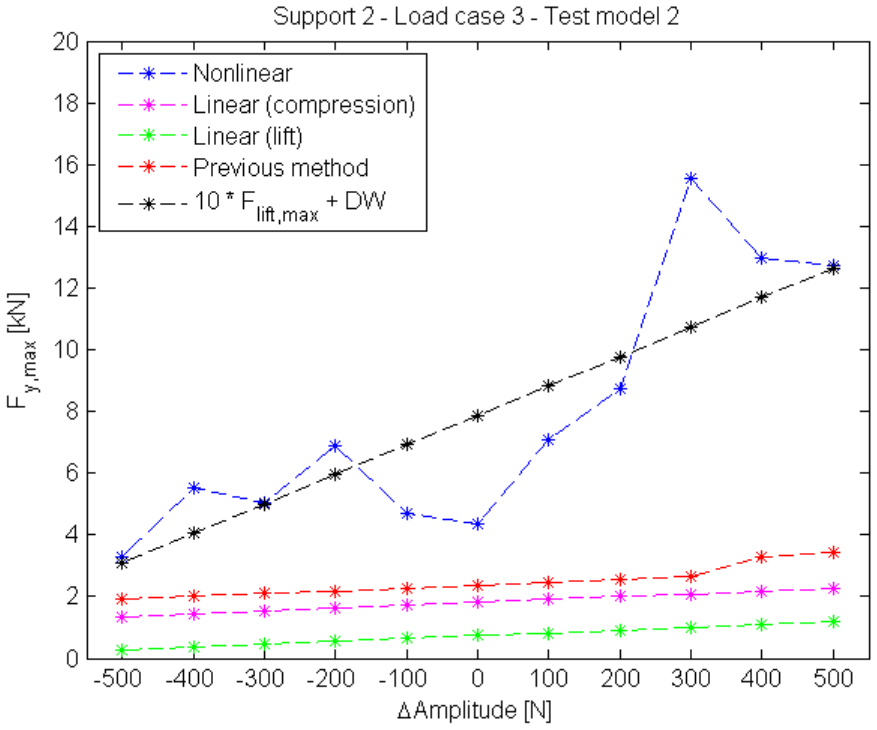

Figure 9.9: Maximum force vs. change of amplitude in load case 3 for support number 2 (test model 2).

9.1.3 Spring support

The ratio between the maximum force from the nonlinear analysis and the corresponding value from the linear analysis are plotted for test model 1 and 2 in figure 9.10 and 9.11. It can be seen that all results are close to or below a value of 1 for both test models, which means that the linear analysis is giving equal or slightly larger/smaller forces compared to the nonlinear analysis.

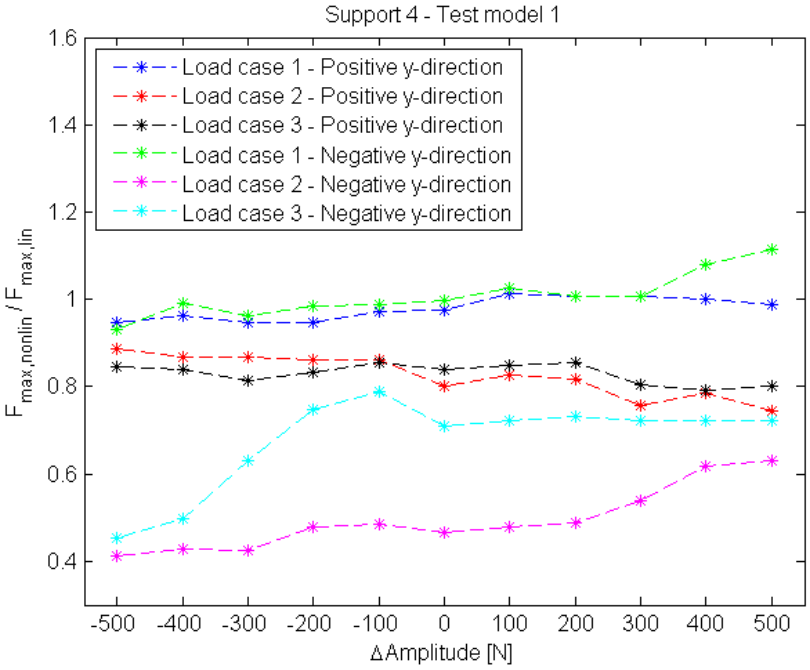

Figure 9.10: Ratio between maximum force calculated with nonlinear and linear analysis for support number 4 (test model 1) when the amplitude is varied.

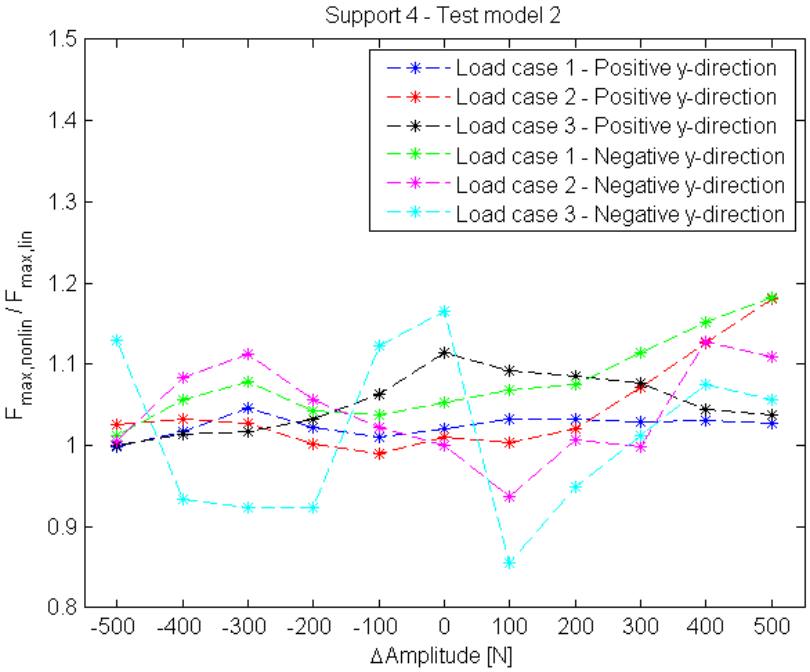

Figure 9.11: Ratio between maximum force calculated with nonlinear and linear analysis for support number 4 (test model 1) when the amplitude is varied.

9.1.4 Pipe run with nonlinear support

How the maximum difference in maximum resultant moment varies with the amplitude can be seen in figure 9.12 and 9.13. The observations that can be made from figure 9.12 and 9.13 are that all load cases show increasing values when the amplitude is increasing and test model 2 is used. When the guide support is modelled as nonlinear instead, it can be noted that the maximum difference for load case 1 is no longer strictly increasing when the amplitude increases. From equation (2.2) that is used to evaluate the stress level in piping systems due to occasional loading, it was seen that the resultant moment was included in one of the terms. This in combination with the results in figure 9.12 and 9.13 implies that a lower stress level will be obtained in at least one node of the piping system, if the maximum resultant moment from the linear analysis is used instead of the value from the nonlinear analysis.

From table 9.1 it can be seen that the elements, in which the maximum difference in maximum resultant moment occurs, is varying quite much depending on which load case that is used. The largest differences between linear and nonlinear analysis are seen in figure 8.3 to occur most in the elements close to the anchor (for test model 1) and near the one-way support (for test model 2).

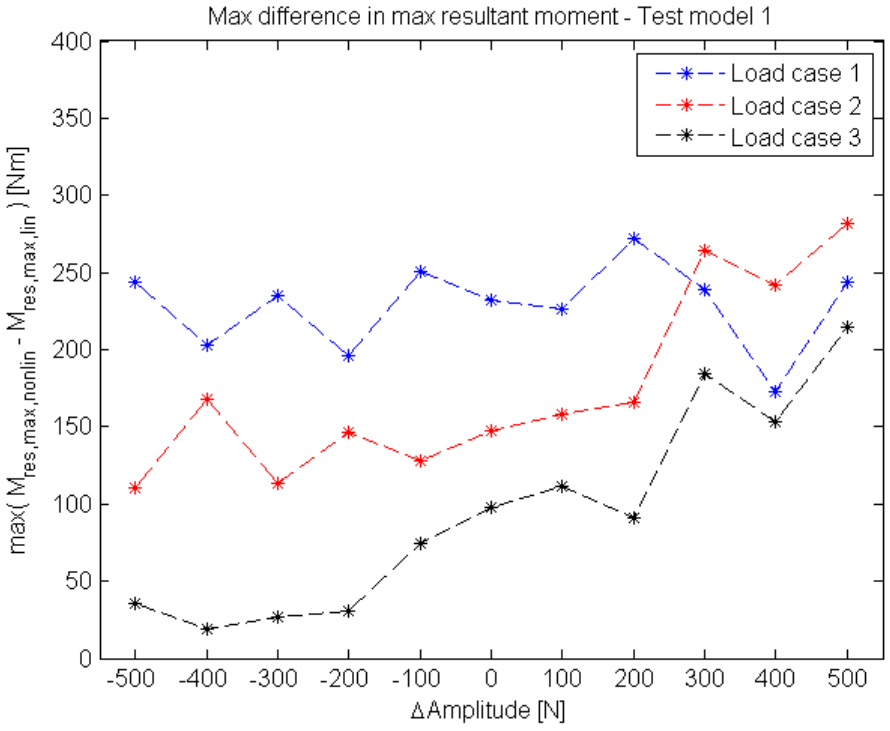

Figure 9.12: Maximum difference in maximum resultant moment when the amplitude of the water hammer load is varied and test model 1 is used.

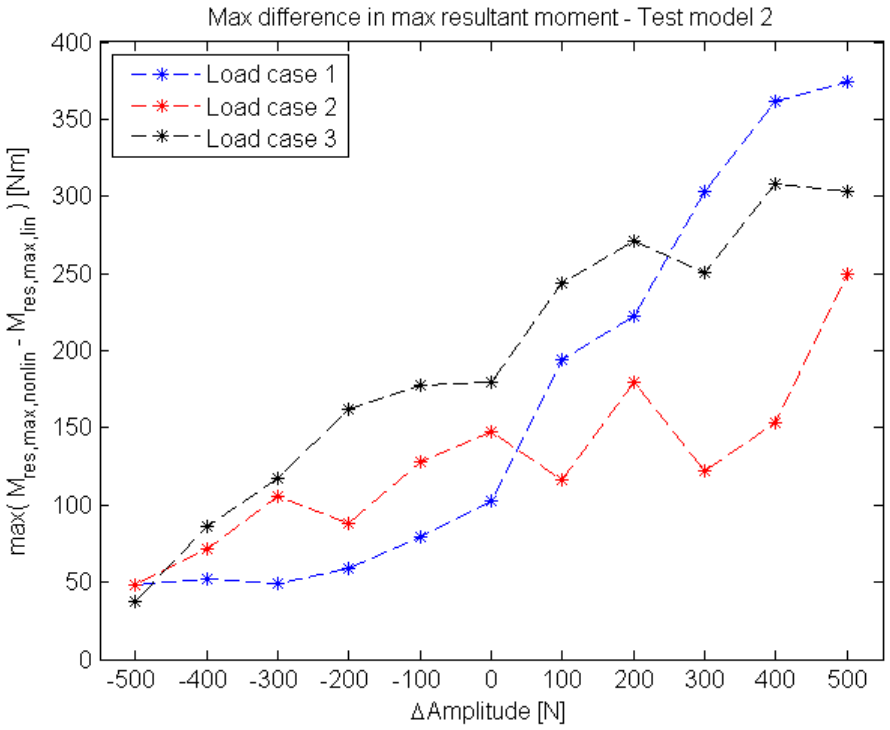

Figure 9.13: Maximum difference in maximum resultant moment when the amplitude of the water hammer load is varied and test model 2 is used.

Table 9.1: Elements in which the maximum difference in maximum resultant moment occurs.

ΔAmplitude [N]	Test model 1			Test model 2		
	Load case 1	Load case 2	Load case 3	Load case 1	Load case 2	Load case 3
-500	83	82	68	71	68	68
-400	83	78	85	83	68	69
-300	77	90	63	83	69	69
-200	79	82	63	72	69	68
-100	83	90	68	71	69	74
0	83	90	68	71	69	69
100	83	90	68	72	69	69
200	77	90	68	71	69	69
300	83	82	68	72	69	73
400	89	83	68	71	69	74
500	80	82	68	71	69	69

9.2 Support stiffness

9.2.1 Guide support

The results from the analyses where the support stiffness has been varied can be seen in figure 9.14 to 9.16 for support number 1. The same results as for the amplitude tests are found in figure 9.14 to 9.16 when considering the approximate maximum force based on the previous method. Use of this method will not give a good approximation for any of the load cases as seen when comparing the red and blue lines in figure 9.14 to 9.16.

In general the results show that an increase in support stiffness gives an increase in maximum force except for load case 1 where the force is seen to decrease when reaching the upper limit for the study. It can also be noted from figure 9.14 to 9.16 that the suggested equations (based on the amplitude tests) can only be used to get a good approximation of the maximum force when the stiffness is varied close to the value used in the amplitude tests (50 kN/mm).

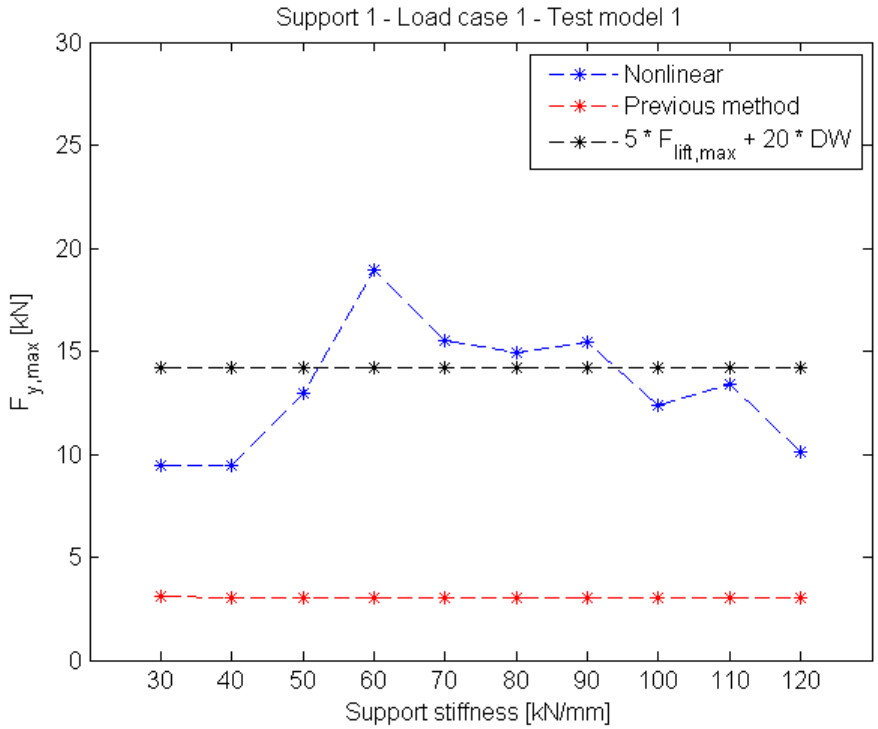

Figure 9.14: Maximum force vs. stiffness for support number 1 when load case 1 is applied.

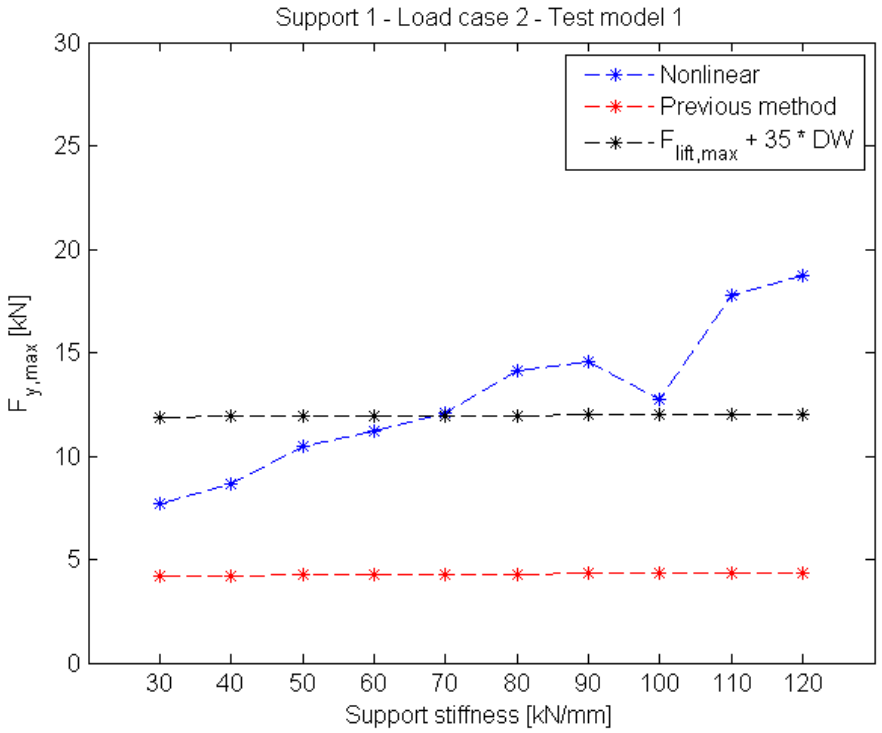

Figure 9.15: Maximum force vs. stiffness for support number 1 when load case 2 is applied.

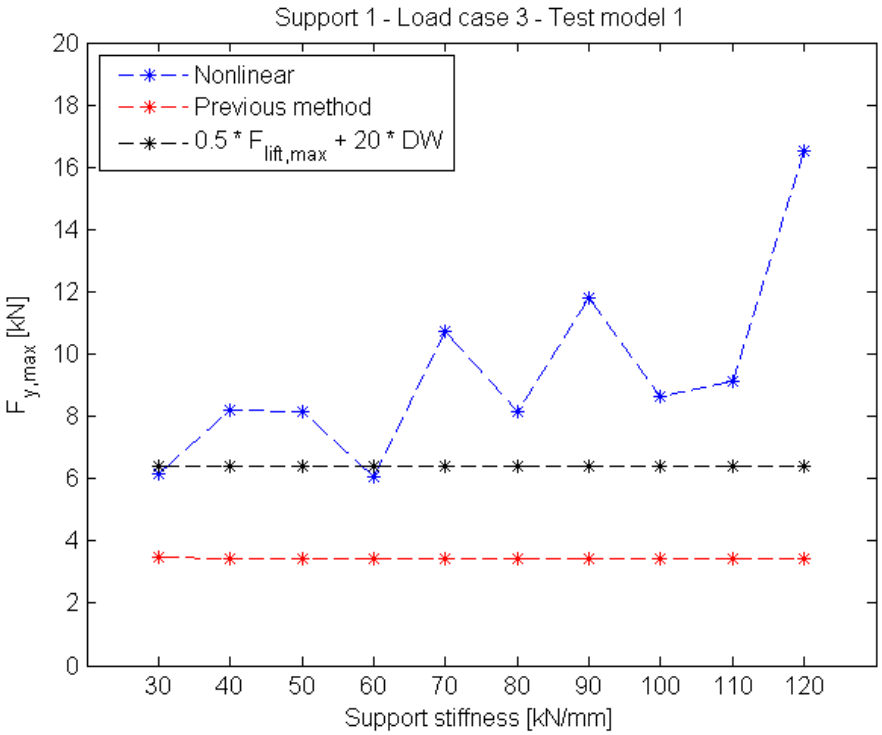

Figure 9.16: Maximum force vs. stiffness for support number 1 when load case 3 is applied.

9.2.2 One-way support

Figure 9.17 to 9.22 show how the maximum force is varying in support number 2 when the support stiffness is varied for the two test models and the three load cases. It is interesting to note that the maximum force from the nonlinear analysis is increasing with increasing support stiffness for all load cases when the gaps in the guide support are neglected. This is not the case for the first load case where the maximum force is seen to decrease when the support stiffness is increased from 90 kN/mm and the gaps are included in the nonlinear analysis.

Use of the previous method to approximate the maximum contact force gives values that are not corresponding to the ones from the nonlinear analysis, except when the stiffness is lowered from its original value (50 kN/mm) and test model 1 is used. Note that the approximate value from the suggested equations in figure 9.18 and 9.20 deviates quite much when higher stiffness than in the amplitude test are used in combination with a piping system containing only one nonlinear support.

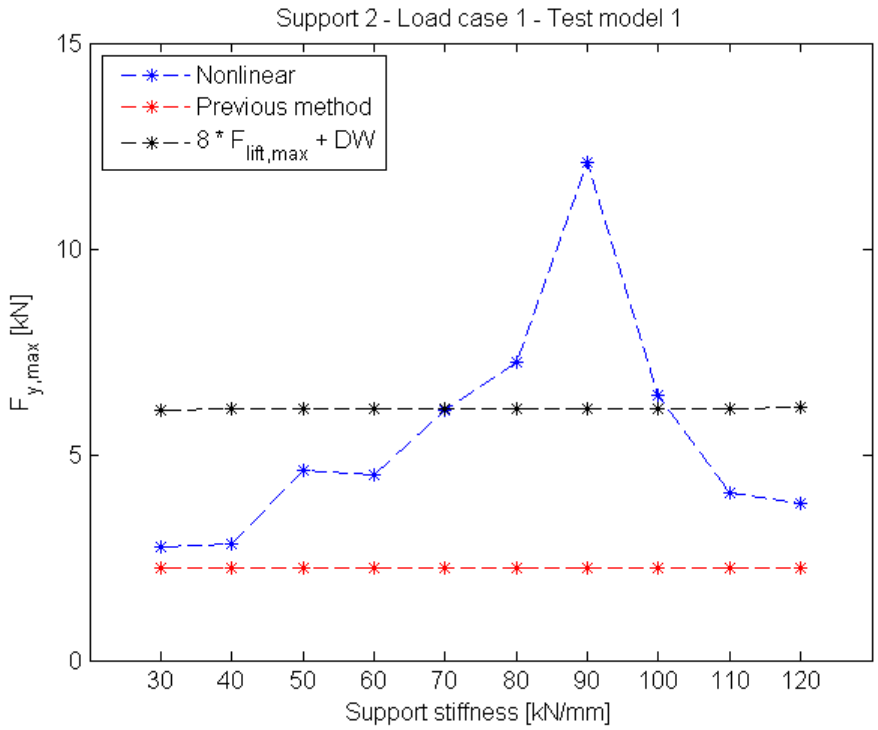

Figure 9.17: Maximum force vs. stiffness for support number 2 (test model 1) when load case 1 is applied.

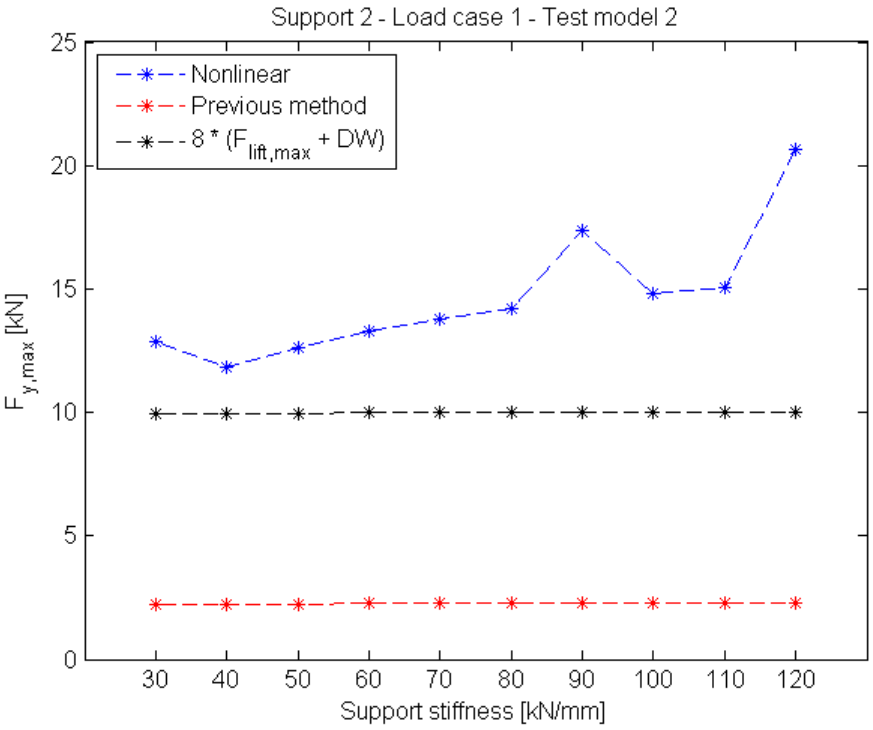

Figure 9.18: Maximum force vs. stiffness for support number 2 (test model 2) when load case 1 is applied.

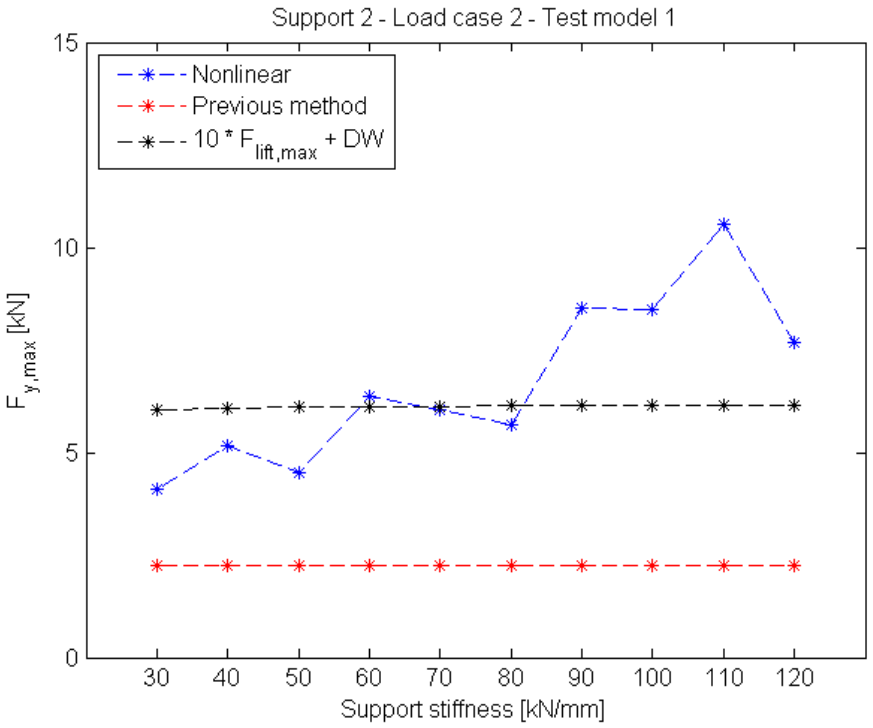

Figure 9.19: Maximum force vs. stiffness for support number 2 (test model 1) when load case 2 is applied.

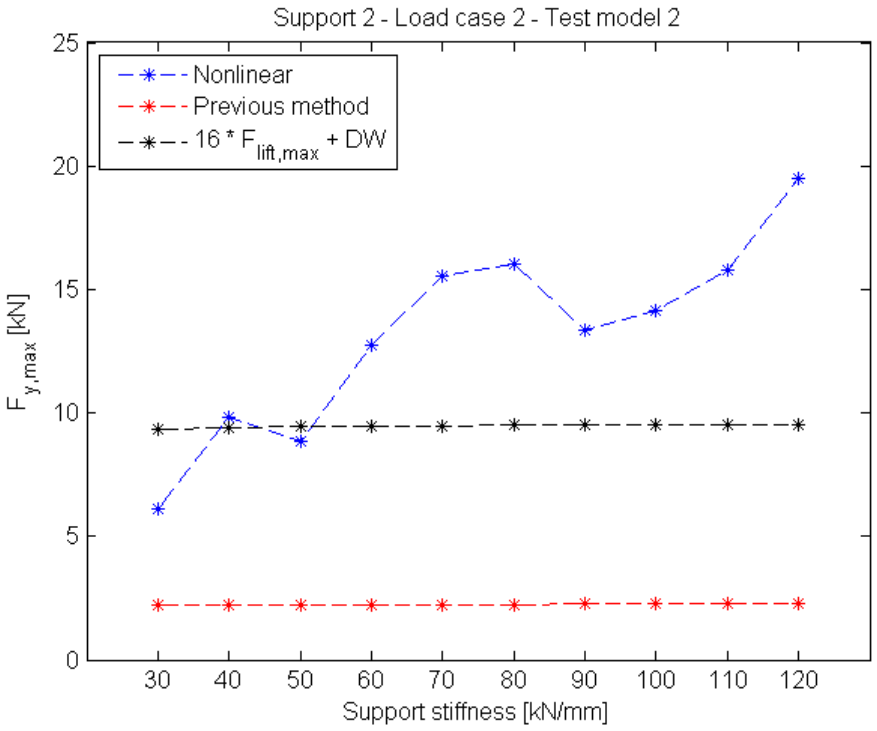

Figure 9.20: Maximum force vs. stiffness for support number 2 (test model 2) when load case 2 is applied.

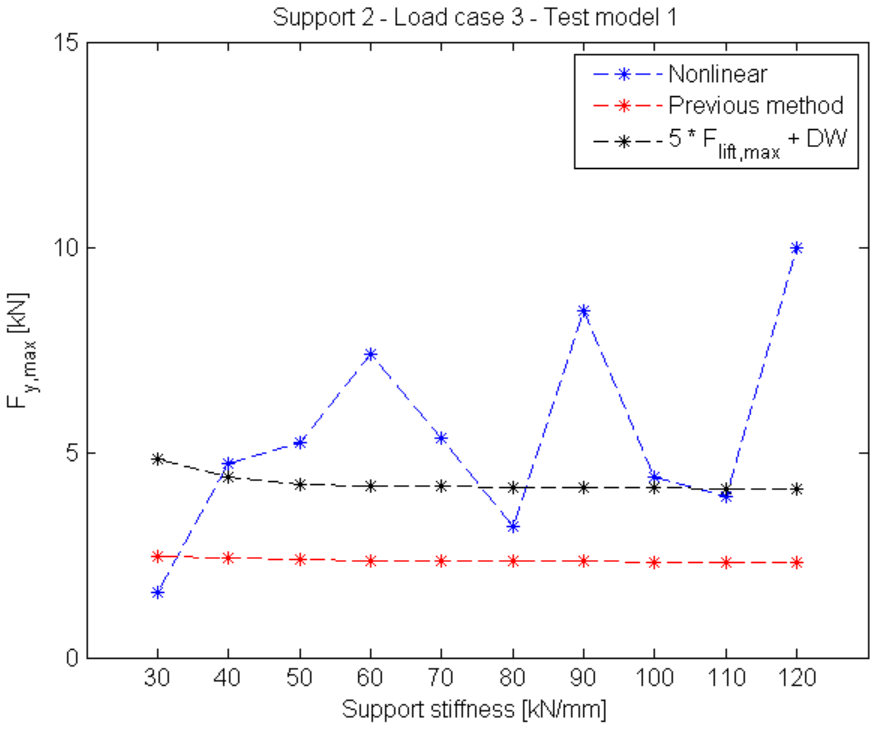

Figure 9.21: Maximum force vs. stiffness for support number 2 (test model 1) when load case 3 is applied.

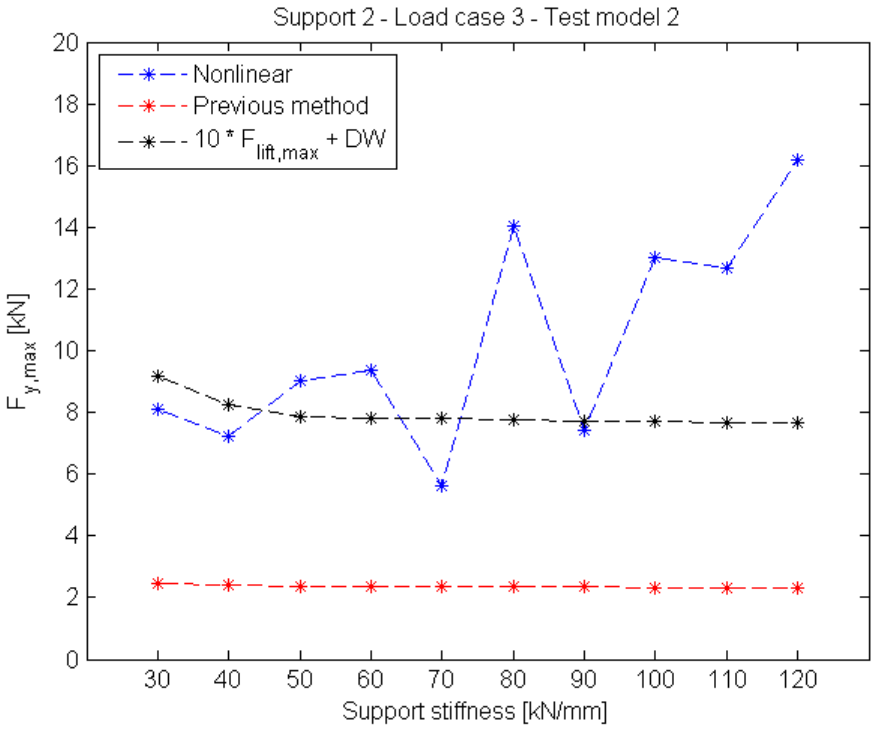

Figure 9.22: Maximum force vs. stiffness for support number 2 (test model 2) when load case 3 is applied.

9.2.3 Spring support

The ratio between maximum force from the nonlinear analysis and the corresponding value from the linear analysis are shown for test model 1 and 2 in figure 9.23 and 9.24 when the support stiffness is varied. The results show that the ratio is below or close to a value of 1, which means that a linear analysis would be possible to use to calculate maximum force in a spring support although the piping system contains nonlinearities. If considering the plot in figure 9.23 for load case 2 in negative y-direction for example, the linear analysis is seen to give a twice as high value as the nonlinear analysis. This indicates that a linear analysis may give conservative values in some cases for linear support types, compared to a nonlinear analysis, although the piping system contains nonlinear supports.

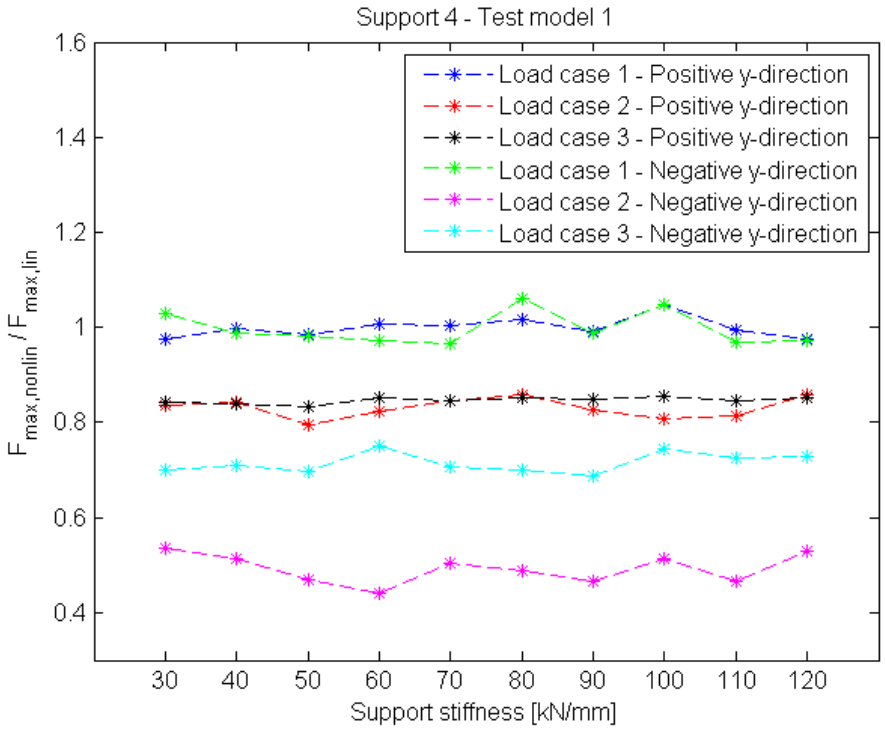

Figure 9.23: Ratio between maximum force calculated with nonlinear and linear analysis for support number 4 (test model 1) when the support stiffness is varied.

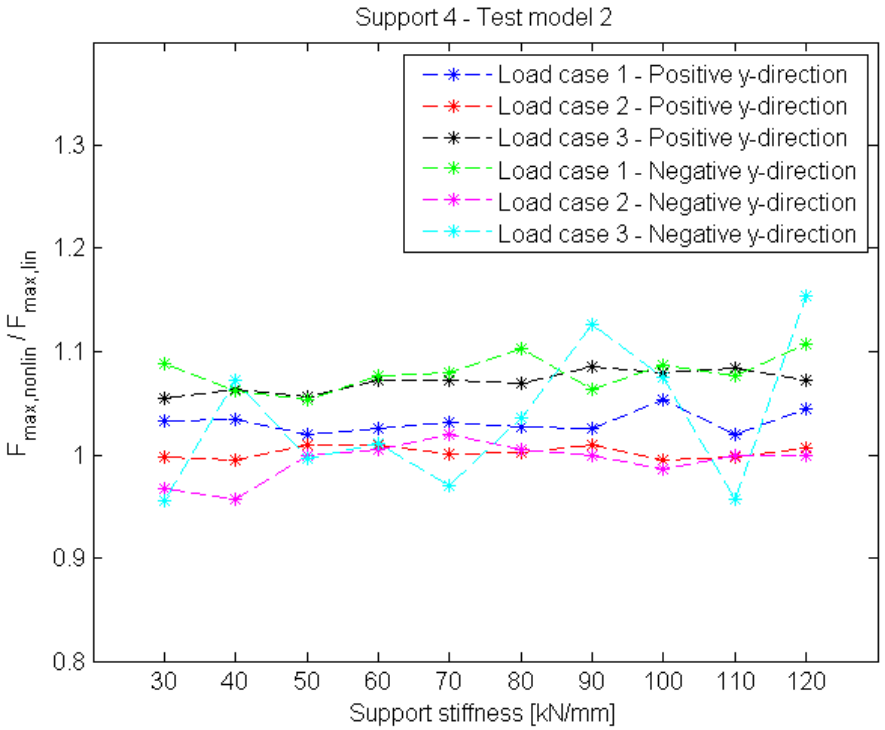

Figure 9.24: Ratio between maximum force calculated with nonlinear and linear analysis for support number 4 (test model 2) when the support stiffness is varied.

9.2.4 Pipe run with nonlinear supports

Figure 9.25 and 9.26 show how the maximum difference in maximum resultant moment is varying with support stiffness for the two test models. For the case with nonlinear modelling of the guide support, the maximum difference is only influenced by the support stiffness when load case 1 is applied. The results also show that the maximum resultant moment become higher in some parts of the piping system when nonlinear analyses are performed, irrespective of which piping system configuration that is considered.

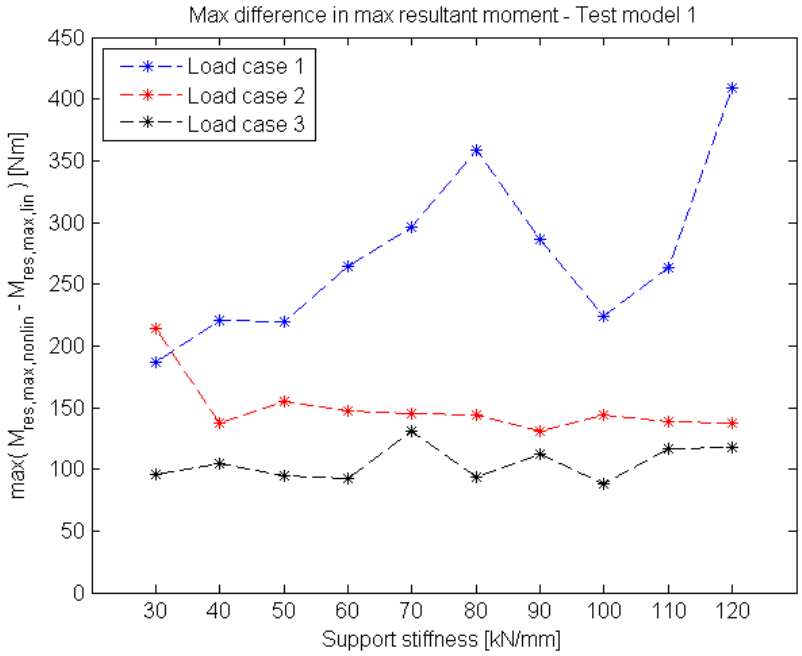

Figure 9.25: Maximum difference in maximum resultant moment when the support stiffness is varied and test model 1 is used.

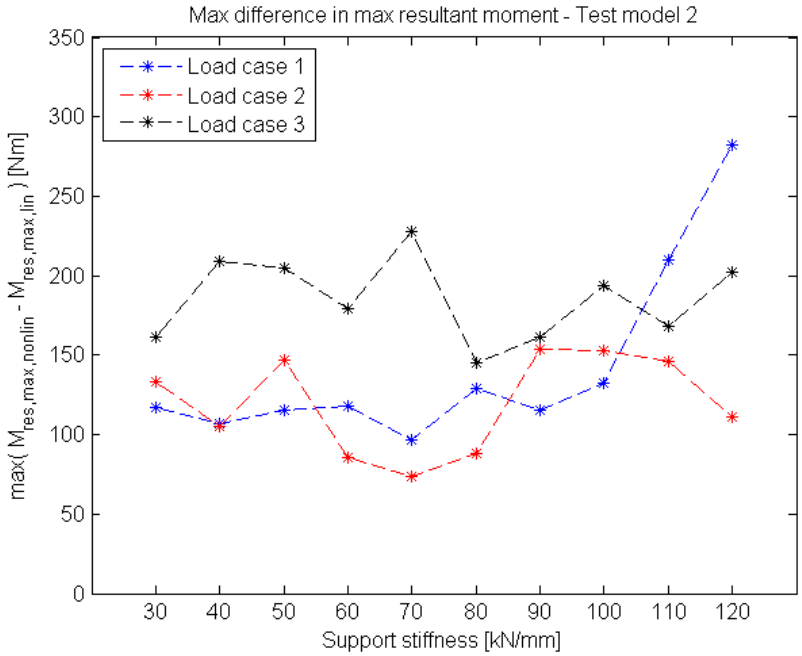

Figure 9.26: Maximum difference in maximum resultant moment when support stiffness is varied and test model 2 is used.

Table 9.2 lists the numbers for the elements in which the maximum difference in maximum resultant moment occurs. From figure 8.3 it is seen that the elements close to the nonlinear supports are achieving the largest difference in maximum resultant moment between linear and nonlinear analysis.

Table 9.2: Elements in which the maximum difference in maximum resultant moment occurs.

Stiffness [kN/mm]	Test model 1			Test model 2		
	Load case 1	Load case 2	Load case 3	Load case 1	Load case 2	Load case 3
30	83	83	68	82	69	69
40	83	81	68	71	69	73
50	83	90	68	72	69	74
60	77	90	68	72	69	73
70	77	90	68	72	69	74
80	77	90	68	71	71	73
90	77	90	68	71	69	68
100	77	90	68	83	69	74
110	77	90	68	71	69	69
120	77	90	68	71	69	69

9.3 Gap size

9.3.1 Guide support

The change in maximum force in support number 1 when the size of the gap is varied (i.e. allowing for different amounts of lift) may be seen for the three load cases in figure 9.27 to 9.29. When considering each of the results, it is seen that an increase in gap size not necessarily corresponds to an increase in maximum support force. It is interesting to note that the suggested equations for approximating the maximum force based on values from the linear analysis are giving quite consistent values with the nonlinear analysis, even when the gap size is varied a few millimetres from its original value (2 mm). It can also be concluded from the results that the previous method cannot be used to approximate the maximum force. This because of the significant deviation from the maximum force values determined from the nonlinear analysis that can be seen in figure 9.27 to 9.29.

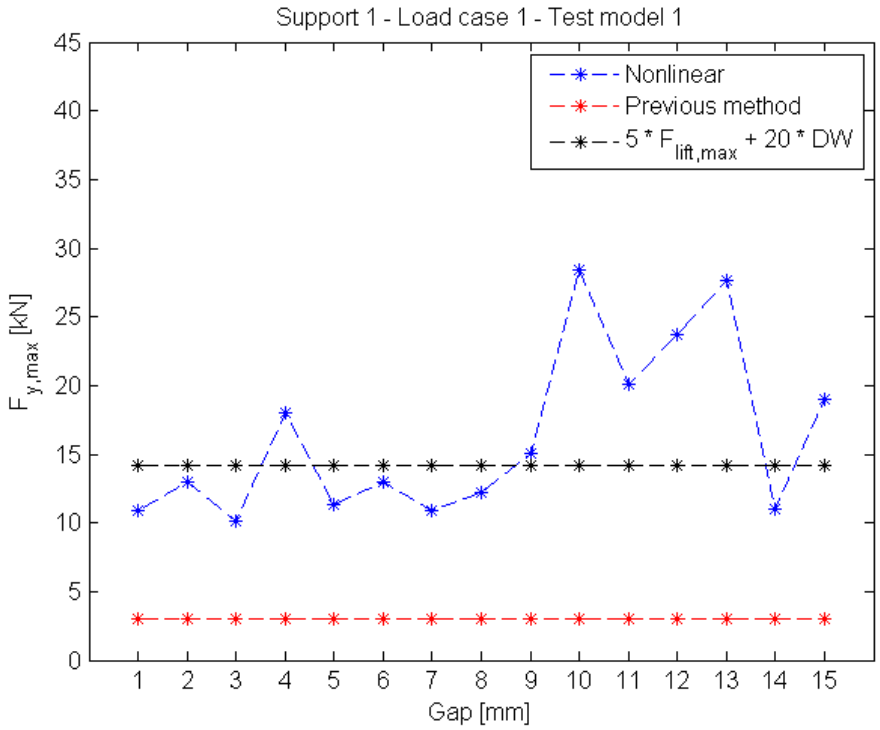

Figure 9.27: Maximum force vs. gap size for support number 1 when load case 1 is applied.

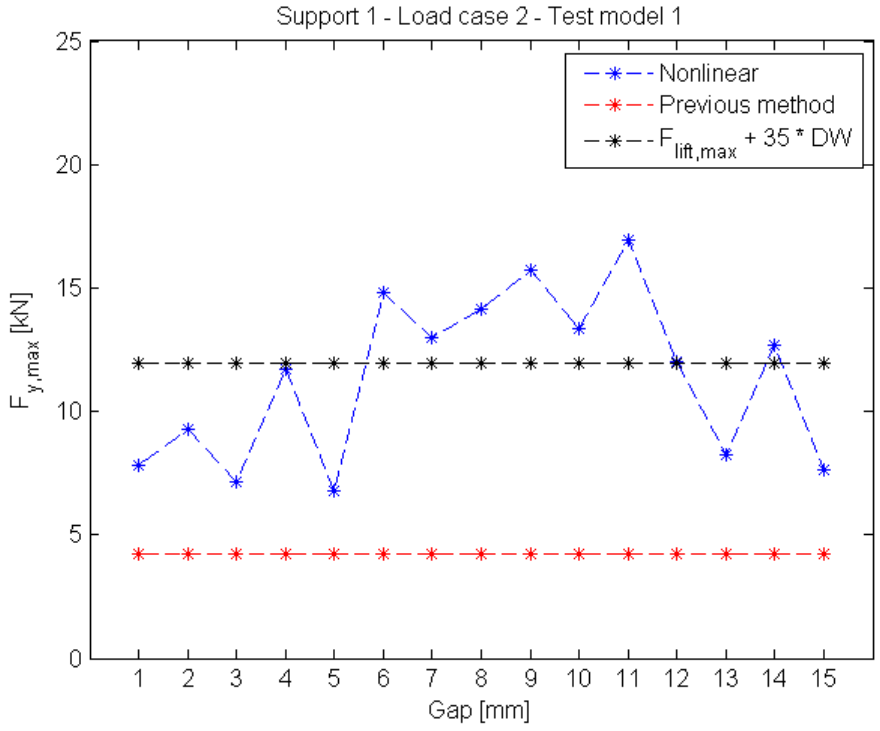

Figure 9.28: Maximum force vs. gap size for support number 1 when load case 2 is applied.

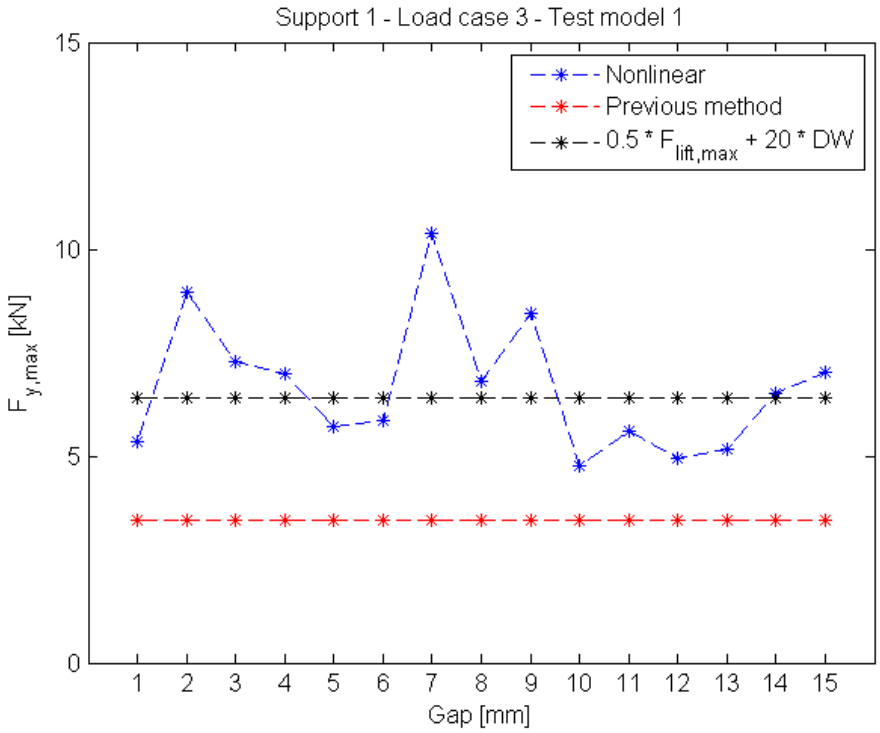

Figure 9.29: Maximum force vs. gap size for support number 1 when load case 3 is applied.

9.3.2 One-way support

The variation in maximum force in the one-way support with the size of the gap in the guide support is presented in figure 9.30 to 9.32. From figure 9.30 to 9.32 it can be seen that the suggested equations are approximating the maximum force very close to the values from the nonlinear analysis, at least up to a gap size of 5 mm. The first load case is most influenced by the gap size since the results are fluctuating more for this load case than compared to the other two load cases. Comparing the maximum force determined from the previous method (red line) and the values calculated by the nonlinear analyses (blue line) shows that the deviation is quite significant in all load cases and for most gap sizes.

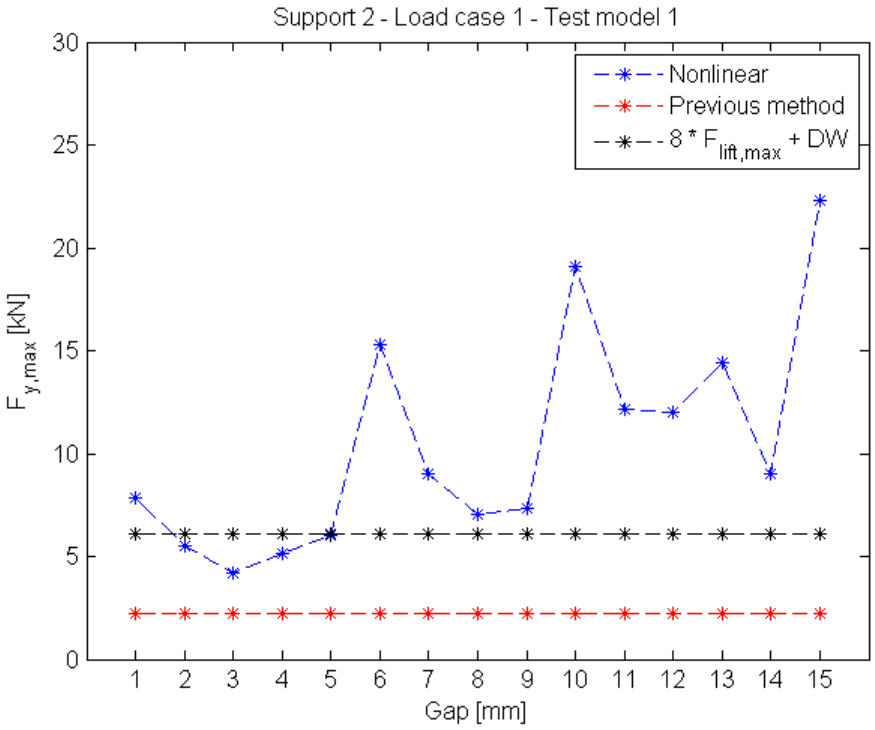

Figure 9.30: Maximum force vs. gap size for support number 2 when load case 1 is applied.

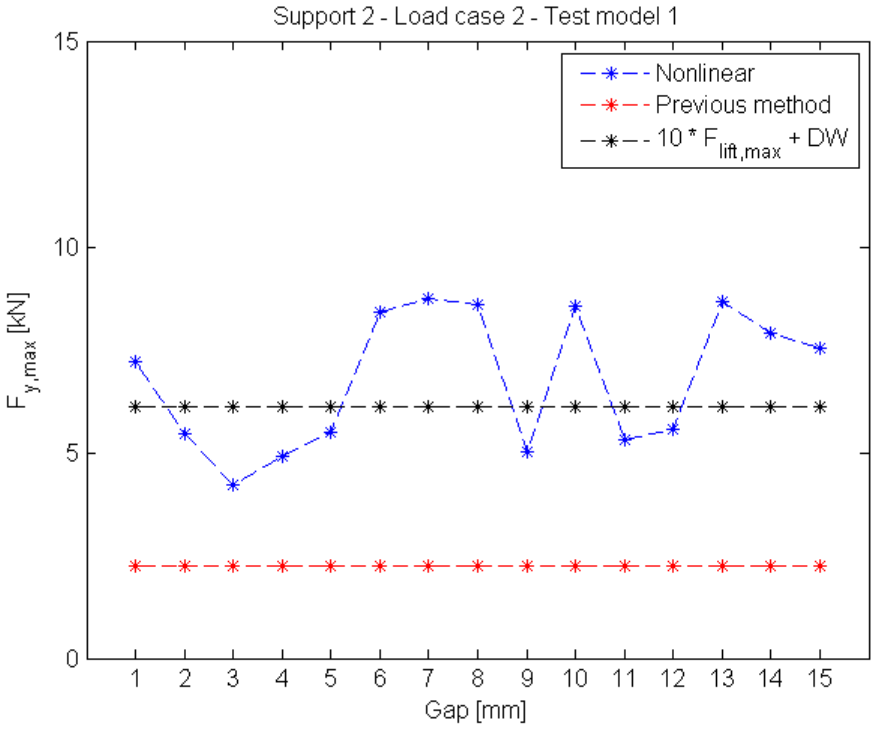

Figure 9.31: Maximum force vs. gap size for support number 2 when load case 2 is applied.

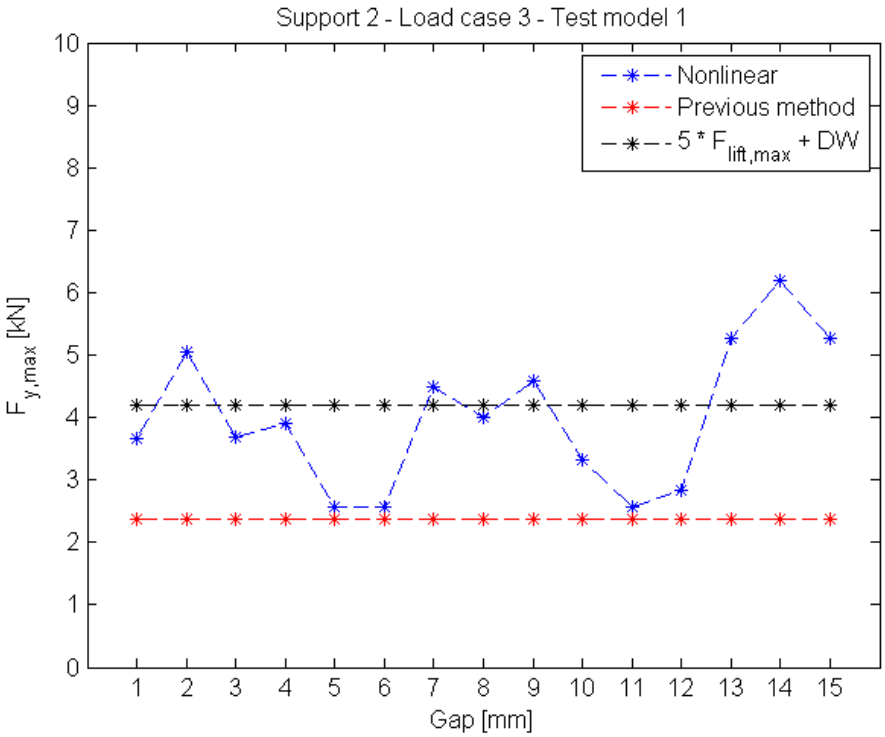

Figure 9.32: Maximum force vs. gap size for support number 2 when load case 3 is applied.

9.3.3 Spring support

Figure 9.33 shows the ratio between the maximum force in support number 4 determined from the nonlinear analysis and the corresponding value from the linear analysis, when the gap size is varied. The ratio is found to be below or near a value of 1 in all load cases, irrespective of which gap that is used, which is very similar to the results shown for the amplitude (figure 9.10) and stiffness (figure 9.23) tests. This implies that a linear analysis would be acceptable to use to analyse the maximum force in spring supports although the piping system includes nonlinear supports, if somewhat conservative values are acceptable.

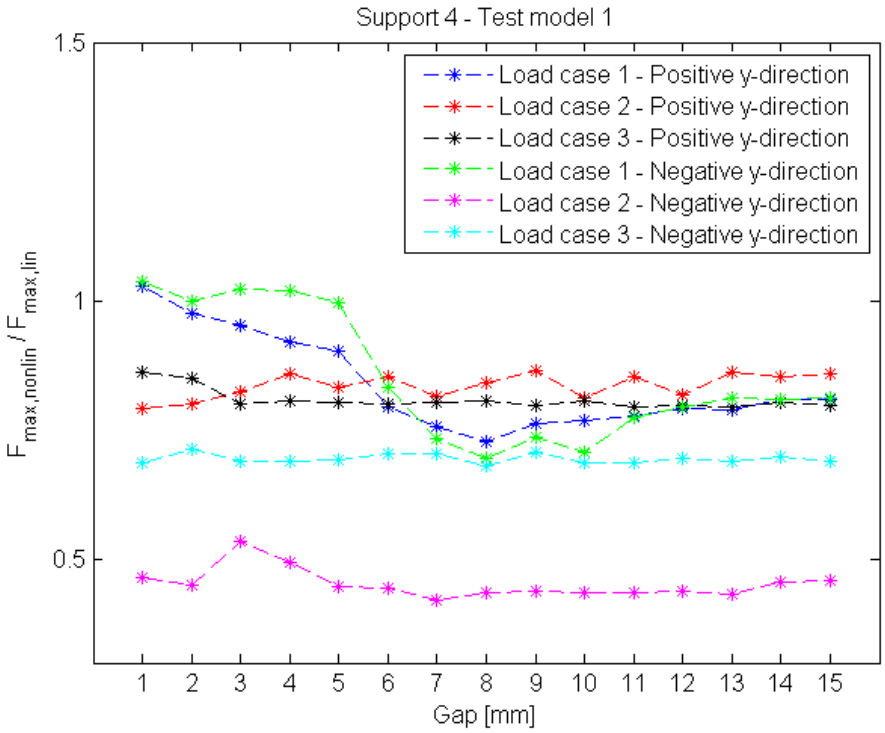

Figure 9.33: Ratio between maximum force calculated with nonlinear and linear analysis for support number 4 when the gap size is varied.

9.3.4 Pipe run with nonlinear supports

Figure 9.34 shows how the maximum difference in maximum resultant moment is varying with the gap size for the three load cases. The first load case is seen to give the largest difference in maximum resultant moment as the gap size is increased. For load case 2 and 3 are the maximum difference near constant throughout the variation of gap size.

It can be noted from table 9.3, which lists the element in which the maximum difference in maximum resultant moment occurs, that the element next to the anchor and the one near the pipe bend before the one-way support are exposed to the largest differences when including nonlinearities in the analysis (see figure 8.3).

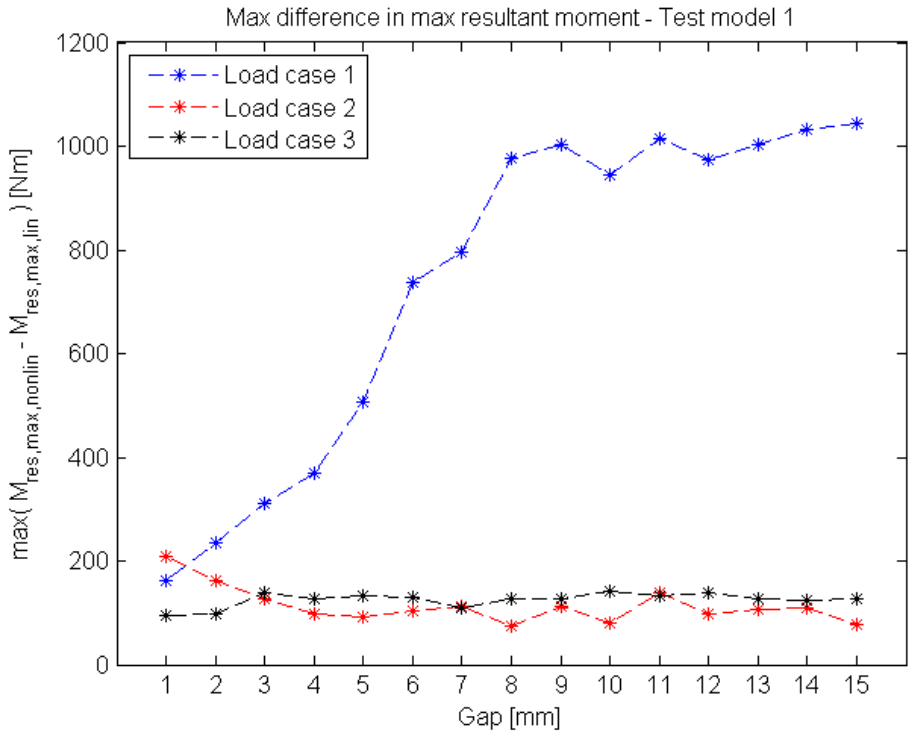

Figure 9.34: Maximum difference in maximum resultant moment when the gap size is varied.

Table 9.3: Elements in which the maximum difference in maximum resultant moment occurs.

Gap [mm]	Load case 1	Load case 2	Load case 3
1	77	82	76
2	83	90	68
3	83	90	68
4	83	68	68
5	83	68	68
6	83	68	68
7	83	68	68
8	83	68	68
9	83	68	68
10	83	76	68
11	83	68	68
12	83	68	68
13	83	68	68
14	83	68	68
15	83	68	68

9.4 Typical piping system

The results for the nonlinear supports in the typical piping system are seen in table 9.4. When comparing the maximum force from the nonlinear analysis with the approximate values from two of the suggested equations for one-way supports, one may note that use of these equations seems to overestimate the maximum force in some of the nonlinear supports where the linear analysis indicates a non-zero lift force. The largest difference is seen to occur in the supports where a high maximum lift force value is determined from the linear analysis.

It is quite interesting that the results show that the previous method now gives an approximation of the maximum force that is closer to the corresponding value from the nonlinear analysis than in the parameter study. This is seen in figure 9.35 which shows the ratio between the approximately calculated maximum force and the actual maximum force from the nonlinear analysis, where the ratio is close to one or slightly higher for most of the nonlinear supports.

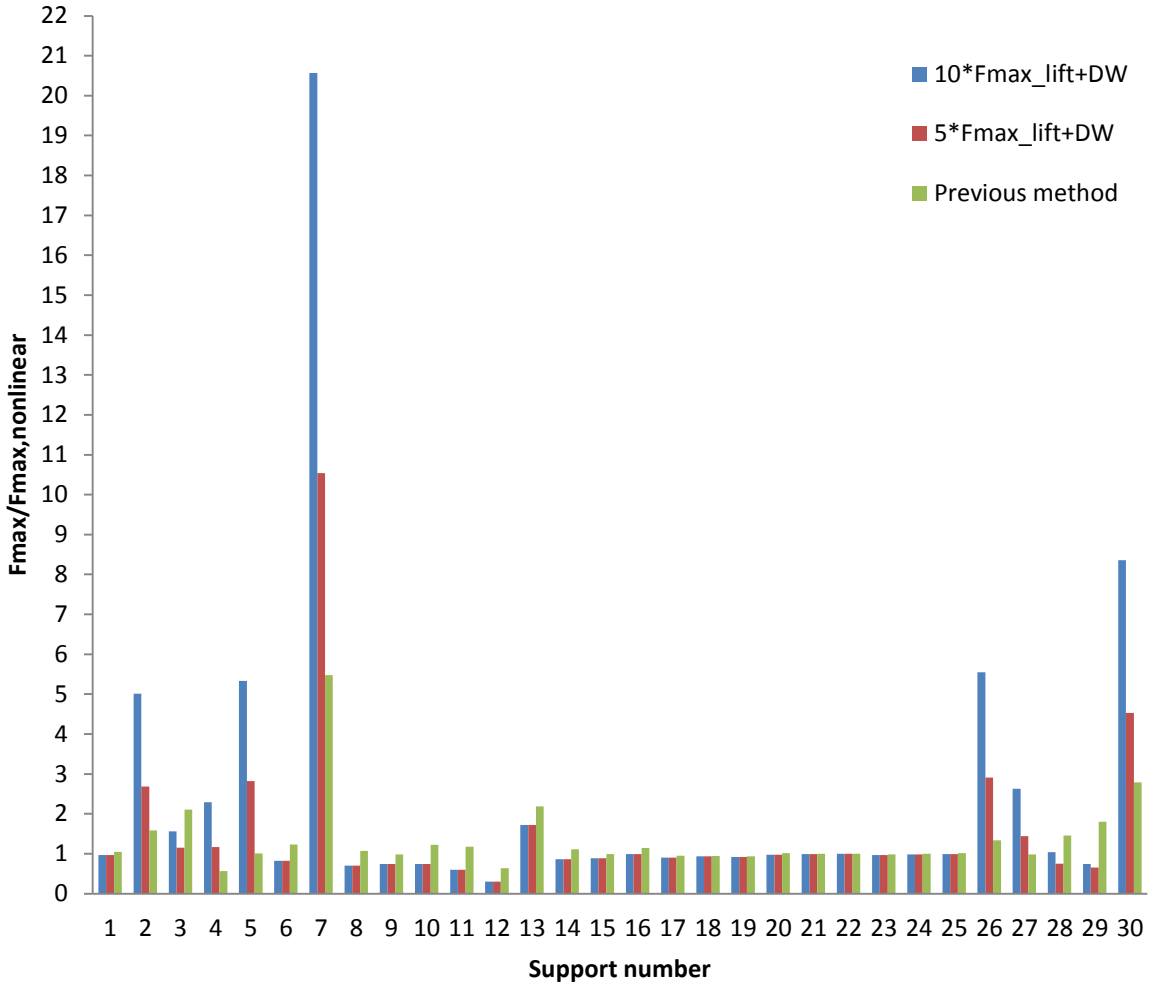

Figure 9.35: Shows the ratio between the approximate maximum force and the corresponding value from the nonlinear analysis.

Table 9.4: Evaluation of the suggested equations and the previous method
(all values are presented in Newton).

DW	$F_{lift,max}$	$F_{comp,max}$[5]	$\frac{F_{lift,max}}{F_{comp,max}}$	$F_{max,nonlinear}$	$F_{max} = k * F_{lift,max} + DW$		Previous method
					k=10	k=5	
585	0	637	0	606	585	585	637
3666	4615	12317	0.37	9948	49812	26739	15798
7929	864	12101	0.07	10602	16570	12249	22340
544	2462	7751	0.32	10983	25168	12856	6194
5462	8637	11548	0.75	17225	91830	48646	17321
840	0	1251	0	1018	840	840	1251
50	199	361	0.55	99	2036	1043	542
383	0	582	0	544	383	383	582
185	0	245	0	250	185	185	245
218	0	360	0	294	218	218	360
324	0	636	0	541	324	324	636
194	0	406	0	640	194	194	406
267	0	339	0	155	267	267	339
206	0	265	0	238	206	206	265
295	0	330	0	334	295	295	330
108	0	125	0	109	108	108	125
361	0	380	0	399	361	361	380
283	0	286	0	303	283	283	286
268	0	272	0	292	268	268	272
112	0	117	0	115	112	112	117
554	0	556	0	558	554	554	556
526	0	528	0	528	526	526	528
166	0	169	0	172	166	166	169
363	0	370	0	370	363	363	370
311	0	318	0	313	311	311	318
313	608	1220	0.50	1152	6396	3354	1540
283	257	753	0.34	1087	2854	1568	1071
303	38	677	0.06	661	686	495	964
253	8	593	0.01	447	332	293	806
293	320	840	0.38	418	3492	1892	1166

[5] Maximum compression force in a nonlinear support when modelled as linear.

10. Discussion and conclusions

The scope of this thesis has been to investigate the possibilities of formulating an equation that can be used to approximate the maximum force in a nonlinear support although the nonlinear support is modelled as linear in the time history analysis. For the one-way support, it was found that use of equation (10.1) gives an approximation of the maximum force that was close to the value from the nonlinear analysis for most cases.

$$F_{max,one-way} = k * F_{max,lift} + DW \tag{10.1}$$

where

$F_{max,one-way}$	Maximum force in a one-way support
$F_{max,lift}$	Maximum lift force
DW	Weight load carried by the support

It turned out from the parameter study, however, that it is not possible to use just one value for the factor k that covers all cases that have been studied. The main reason for this is due to the influence of the frequency content of the water hammer load and the piping system configuration on the response of the piping system. It is certainly no surprise that the frequency content would influence the results in some way but when considering the plots for the guide support for example, it is seen that one load case shows an increase in maximum force while another load case shows a near constant maximum value as the parameter value is varied.

When comparing the results for the two test models, it was found that a higher maximum reaction force was obtained for the piping system containing one nonlinear support compared to the other system with two nonlinear supports. This may be part of the explanation why the suggested equations are overestimating the maximum force in some of the nonlinear supports compared to the results from the nonlinear analysis of the typical piping system. When considering the results for the typical piping system, it was noted that use of the previous method gives an approximation that is closer to the corresponding value from the nonlinear analysis than the suggested equations. This was unexpected since the parameter variations indicated that this method did not confirm that well to the results from the nonlinear analyses. Further, for some of the nonlinear supports where linear modelling gives a lift force greater than zero, the maximum compression force was found to be greater than the maximum reaction force from the nonlinear analysis. This result is very interesting since it was thought that a lift force greater than zero would result in a maximum reaction force that is larger when nonlinearities are accounted for in the analysis than when neglected.

The largest difference in maximum resultant moment between linear and nonlinear analysis was found to occur when the load case with low frequency content was applied. Especially the analyses where the gap size was varied showed that the error could be expected to increase almost linearly with the gap. The maximum error was occurring in the elements close to where the anchor is positioned or in the elements near the guide and one-way support for most of the tests. This is in agreement since the anchor is a rigid support that should transfer a great part of the load on the piping system and nonlinear modelling of the nonlinear supports allows for more flexibility which is thought to lead to greater torsional and bending moments than in case of linear modelling.

The parameter study and the analyses of a typical piping system with real time history loading have shown that it is quite difficult to propose an equation or method that compensates for nonlinear effects which have been neglected in the linear time history analysis of a nonlinear piping system. For this reason, it is recommended that nonlinear supports are modelled as nonlinear when performing time history analysis if more accurate results are required.

10.1 Further work

A suggestion for further work is to use the ASME BPVC evaluation toolbox [4] that has been developed for use in ANSYS to study how the stress levels in a nonlinear piping system is influenced by the modelling of nonlinear supports. From the results of the parameter study, it was shown that the difference in maximum resultant moment between the linear and nonlinear analysis was significant and should be considered. For that reason and because the resultant moment is used in equation (2.2) to evaluate the stress ratio in the piping system, this is of interest to investigate more in detail.

In this thesis, just some of the important parameters in a nonlinear piping system have been studied. One may for instance consider the solution of the equations of motion. It was mentioned in the time history analysis section that two methods can be used to solve the equations of motion. In this thesis has only direct time integration been considered but it could be interesting to perform test where mode superposition is used instead to study whether this influences the forces and moments. With mode superposition it is possible to use modal (constant) damping which gives an opportunity to also study how the damping modelling is influencing the results.

References

[1] Smith P.R. & Van Laan T.J., *Piping and pipe support systems*, McGraw-Hill, 1987

[2] Lüdecke H.J. & Kothe B., *Know-how Volume 1: Water hammer*, KSB, 2006

[3] Ottosen N.S. & Peterson H., *Introduction to the Finite Element Method*, Prentice Hall, 1992

[4] Andersson H., *Code evaluation of nonlinear piping systems*, Master thesis, Lund University, 2011

[5] Krenk S., *Non-linear Modeling and Analysis of Solids and Structures*, Cambridge University Press, 2009

[6] Björndahl O., *Guidelines for design for analysis and design review of nuclear class 1 and 2 piping systems*, DNV RSE R&D Report No. 2002/05, revision 0, 2002

[7] ANSYS release 14.5 documentation

[8] Sundström B., *Handbok och formelsamling i Hållfasthetslära*, KTH, 2010

[9] Axelsson J. & Viktorsson H., *Influence of Support Stiffness in Dynamic Analysis of Piping Systems*, Master thesis, Chalmers University of Technology, 2011

Appendix

A.1 The previous method

This method uses the maximum lift force $F_{lift,max}$ and maximum compression force $F_{comp,max}$ from a linear time history analysis of the nonlinear piping system to determine which of the two equations in (A.1) that should be used to approximately calculate the maximum force in a nonlinear support when $F_{lift,max} > 0$

$$\begin{cases} F_{max} = 2 * (DW + TE) + F_{dyn} & \text{if} \quad F_{lift,max} < 0.5F_{comp,max} \\ F_{max} = 1.5 * \left|F_{max,dyn}\right| & \text{if} \quad F_{lift,max} \geq 0.5F_{comp,max} \end{cases} \tag{A.1}$$

where DW and TE is the weight and thermal expansion load sustained by the support.

To illustrate the method consider figure A.1. First are the static loads in terms of dead weight and thermal expansion applied to the system which in this case gives a total static load equal to $DW + TE_{T_1}$ or $DW + TE_{T_2}$ depending on the operating temperature. Then are the dynamic (time-varying) loads applied to the system which results in different ratios between maximum lift $F_{lift,max}$ and compression force $F_{comp,max}$ depending on which of the two temperatures that are considered.

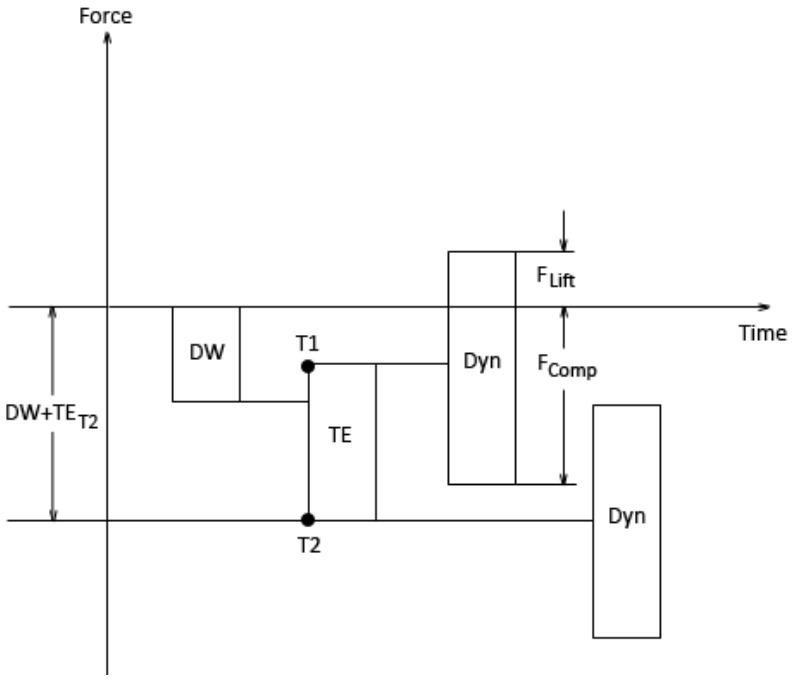

Figure A.1: Loads involved in a time history analysis.

The previous method now suggests that if the maximum lift force is greater than half of the maximum compression force, the maximum force in a one-way support can be approximately calculated by multiplying the maximum dynamic load by a factor of 1.5. If the opposite holds, then the maximum force in a one-way support should instead be calculated by adding two times the static loads to the dynamic load determined by

$$F_{dyn} = \frac{F_{lift,max} + F_{comp,max}}{2} \tag{A.2}$$

A.2 Modal analysis

The eigenfrequencies calculated for the two test models in the range from 0-100 Hz are shown in table A.1 below.

Table A.1: Eigenfrequencies for the two test piping systems.

Mode number	Frequency [Hz]	Mode number	Frequency [Hz]
1	2.73	19	34.36
2	5.88	20	34.63**
3	7.70*	21	37.43
4	8.97*	22	41.77
5	9.46*	23	42.39
6	11.27	24	45.43
7	11.42	25	50.81***
8	15.97*	26	55.76
9	16.97*	27	57.93**
10	19.67	28	59.27
11	21.24	29	69.41***
12	21.40	30	70.64
13	24.07**	31	75.36
14	25.04	32	84.59
15	25.47***	33	86.92
16	25.85	34	89.52
17	27.25**	35	93.79
18	31.40		

* Frequencies included in the frequency content of the water hammer load case 1

** Frequencies included in the frequency content of the water hammer load case 2

** Frequencies included in the frequency content of the water hammer load case 3